Title

Simian Immunodeficiency Virus Targeting of CXCR3+ CD4+ T Cells in Secondary Lymphoid Organs Is Associated with Robust CXCL10 Expression in Monocyte/Macrophage Subsets

Permalink

https://escholarship.org/uc/item/1701s0z0

Journal

Journal of Virology, 91(13)

ISSN

0022-538X

Authors

Fujino, Masayuki
Sato, Hirotaka
Okamura, Tomotaka
et al.

Publication Date

2017-07-01

DOI

10.1128/jvi.00439-17

Peer reviewed

Simian Immunodeficiency Virus Targeting of CXCR3+ CD4+ T Cells in Secondary Lymphoid Organs Is Associated with Robust CXCL10 Expression in Monocyte/Macrophage Subsets

Masayuki Fujino,[a] Hirotaka Sato,[a,b*] Tomotaka Okamura,[b] Akihiko Uda,[c]
Satoshi Takeda,[a] Nursarat Ahmed,[a,b*] Shigeyuki Shichino,[d] Teiichiro Shiino,[e]
Yohei Saito,[a,b*] Satoru Watanabe,[a,b*] Chie Sugimoto,[f*] Marcelo J. Kuroda,[f]
Manabu Ato,[g] Yoshiyuki Nagai,[h] Shuji Izumo,[i] Kouji Matsushima,[d]
Masaaki Miyazawa,[j] Aftab A. Ansari,[k] Francois Villinger,[k,l*] ⓘ Kazuyasu Mori[a,b]

AIDS Research Center,[a] Department of Veterinary Science,[c] Infectious Diseases Surveillance Center,[e] and Department of Immunology,[g] National Institute of Infectious Diseases, Tokyo, Japan; Tsukuba Primate Research Center, National Institutes of Biomedical Innovation, Health and Nutrition, Tsukuba, Ibaraki, Japan[b]; Department of Molecular Preventive Medicine, Graduate School of Medicine, The University of Tokyo, Tokyo, Japan[d]; Division of Immunology, Tulane National Primate Research Center, Tulane University, Covington, Louisiana, USA[f]; Center of Research Network for Infectious Diseases, Riken, Tokyo, Japan[h]; Molecular Pathology, Center for Chronic Viral Diseases, Graduate School of Medical and Dental Sciences, Kagoshima University, Kagoshima, Japan[i]; Department of Immunology, Kindai University School of Medicine, Osaka-Sayama, Osaka, Japan[j]; Department of Pathology and Laboratory Medicine[k] and Yerkes National Primate Research Center,[l] Emory University, Atlanta, Georgia, USA

ABSTRACT Glycosylation of Env defines pathogenic properties of simian immunodeficiency virus (SIV). We previously demonstrated that pathogenic SIVmac239 and a live-attenuated, quintuple deglycosylated Env mutant (Δ5G) virus target CD4+ T cells residing in different tissues during acute infection. SIVmac239 and Δ5G preferentially infected distinct CD4+ T cells in secondary lymphoid organs (SLOs) and within the lamina propria of the small intestine, respectively (C. Sugimoto et al., J Virol 86: 9323–9336, 2012, https://doi.org/10.1128/JVI.00948-12). Here, we studied the host responses relevant to SIV targeting of CXCR3+ CCR5+ CD4+ T cells in SLOs. Genome-wide transcriptome analyses revealed that Th1-polarized inflammatory responses, defined by expression of CXCR3 chemokines, were distinctly induced in the SIVmac239-infected animals. Consistent with robust expression of CXCL10, CXCR3+ T cells were depleted from blood in the SIVmac239-infected animals. We also discovered that elevation of CXCL10 expression in blood and SLOs was secondary to the induction of CD14+ CD16+ monocytes and MAC387+ macrophages, respectively. Since the significantly higher levels of SIV infection in SLOs occurred with a massive accumulation of infiltrated MAC387+ macrophages, T cells, dendritic cells (DCs), and residential macrophages near high endothelial venules, the results highlight critical roles of innate/inflammatory responses in SIVmac239 infection. Restricted infection in SLOs by Δ5G also suggests that glycosylation of Env modulates innate/inflammatory responses elicited by cells of monocyte/macrophage/DC lineages.

IMPORTANCE We previously demonstrated that a pathogenic SIVmac239 virus and a live-attenuated, deglycosylated mutant Δ5G virus infected distinct CD4+ T cell subsets in SLOs and the small intestine, respectively (C. Sugimoto et al., J Virol 86:9323–9336, 2012, https://doi.org/10.1128/JVI.00948-12). Accordingly, infections with SIVmac239, but not with Δ5G, deplete CXCR3+ CCR5+ CD4+ T (Th1) cells during the primary infection, thereby compromising the cellular immune response. Thus, we hypothesized that distinct host responses are elicited by the infections with two different viruses. We

found that SIVmac239 induced distinctly higher levels of inflammatory Th1 responses than Δ5G. In particular, SIVmac239 infection elicited robust expression of CXCL10, a chemokine for CXCR3$^+$ cells, in CD14$^+$ CD16$^+$ monocytes and MAC387$^+$ macrophages recently infiltrated in SLOs. In contrast, Δ5G infection elicited only modest inflammatory responses. These results suggest that the glycosylation of Env modulates the inflammatory/Th1 responses through the monocyte/macrophage subsets and elicits marked differences in SIV infection and clinical outcomes.

KEYWORDS CD4$^+$ T cell, CXCL10, CXCR3, SIV, Th1, glycosylation, innate immunity, macrophages, monocytes, pathogenesis

Human immunodeficiency virus/simian immunodeficiency virus (HIV/SIV) preferentially infect CCR5$^+$ CD4$^+$ T cells in mucosal and systemic immune tissues during primary infection (1, 2). However, in addition to CCR5 expression, the CD4$^+$ T cells are comprised of a diverse population of phenotypically and functionally distinct subsets that include cells classified as Th1, Th2, Th17, follicular T helper (Tfh), and T regulatory (Treg) cells (3). Each subset produces distinct cytokines for specialized helper and/or regulatory functions and expresses, on their cell surfaces, distinct chemokine receptors that help guide migration of these subsets to distinct niches in tissues. Most, if not all, of these CD4$^+$ T cell subsets are either directly or indirectly affected by HIV/SIV infection (1, 4–6). While considerable advances have been made in identification of the subsets of CD4$^+$ T cells that are associated with pathogenesis of HIV/SIV infection, it is not clear how distinct CD4$^+$ T cell subsets are preferentially infected in distinct clinical outcomes (7–9). More importantly, the molecular mechanisms for such selective subset targeting remain to be defined.

We have previously reported that while SIVmac239 infects CD4$^+$ T cells within the T and B cell zones of lymph nodes (LNs) during primary infection in rhesus macaques, a live-attenuated *nef* mutant (ΔNef) virus selectively infects CD4$^+$ T cells localized to the germinal centers/B cell zones, where Tfh cells reside (10). These results highlighted the critical roles of the Nef protein in targeting CD4$^+$ T cells in the paracortex/T cell zones, where CXCR3$^+$ CD4$^+$ T cells are activated and differentiate into Th1 and other CD4$^+$ T cell subsets. Similarly, glycosylation of Env also plays an important role in the targeting of CD4$^+$ T cell subsets.

This conclusion was reached with studies that utilized a series of deglycosylation mutant viruses, in which one to five N-glycosylation sites in the gp120 were mutated (11, 12). We discovered that infection of rhesus macaques with a quintuple deglycosylation mutant (Δ5G) possesses novel properties; thus, whereas Δ5G replicated *in vivo* robustly and to similar levels as SIVmac239 during primary infection, Δ5G-infected monkeys controlled viremia to undetectable levels that lasted >10 years. Such infection with Δ5G conferred significant protection against a challenge infection with the heterologous SIVsmE543-3 (13). The containment of the chronic infection in Δ5G-infected animals was not due to the generation of neutralizing antibodies (14).

These findings led us to focus our interest on defining the host responses that lead to the opposing clinical outcomes between SIVmac239- and Δ5G-infected animals. Our initial findings indicated that while SIVmac239 targets Th1 cells and other CD4$^+$ T cell subsets in secondary lymphoid organs (SLOs), Δ5G preferentially infects CD4$^+$ T cells, most likely Th17 cells, in the lamina propria of the small intestine (1). Collectively, glycosylation of Env and the presence of Nef are required for SIVmac239 targeting of Th1, Tfh, and other CD4$^+$ T cell subsets in SLOs, while infection with either of the two attenuated viruses results in the preservation of CXCR3$^+$ CCR5$^+$ CD4$^+$ T cells in SLOs.

Hence, we now focus on host responses that may determine the opposing clinical outcomes from infection with SIVmac239 or Δ5G. In particular, we studied the expression of CXCR3 chemokines in an effort to elucidate the mechanisms that enable SIVmac239, but not Δ5G, to target CD4$^+$ T cells in SLOs.
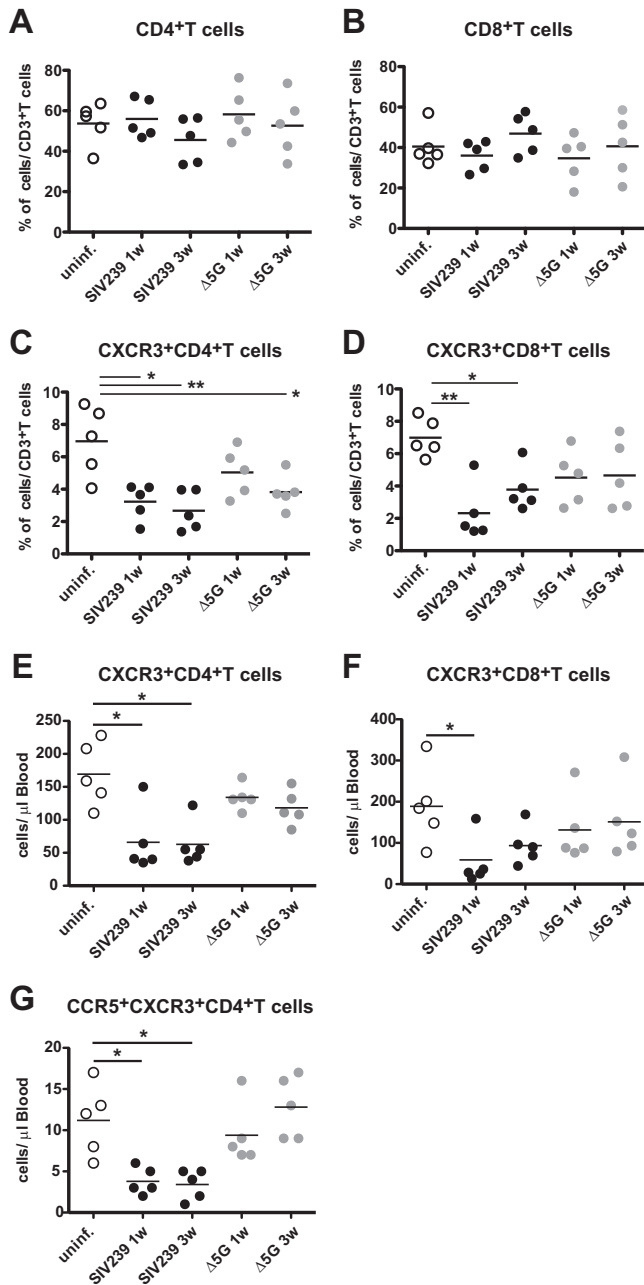
FIG 1 Frequencies of CXCR3-expressing CD4$^+$ T and CD8$^+$ T cells in uninfected, SIVmac239-infected, and Δ5G-infected animals. The frequencies of CXCR3-expressing CD4$^+$ and CD8$^+$ T cells in the gated population of CD3$^+$ T cells (A to D) and the absolute numbers (cell number per microliter of blood) (E to G) were analyzed at 7 days (1 week [1w]) and 21 days (3 weeks [3w]) p.i. by flow cytometry. Cell populations are as indicated above the panels. *, $P < 0.05$; **, $0.01 < P < 0.05$.

RESULTS

Depletion of CXCR3$^+$ T cell cells occurred in blood from SIVmac239-infected animals but not Δ5G-infected animals at 7 days p.i. Flow cytometric analysis of peripheral blood mononuclear cells (PBMCs) from SIVmac239- and Δ5G-infected animals and uninfected control animals revealed that while there were no detectable differences in the levels of total CD3$^+$ CD4$^+$ and CD3$^+$ CD8$^+$ T cells (Fig. 1A and B), there were significant differences in the CXCR3-expressing subset of each of the two T cell lineages. Enumeration of the absolute numbers of the cells showed that CXCR3-expressing CD4$^+$ T cells and CXCR3-expressing CD8$^+$ T cells were depleted at 1 and 3

weeks postinfection (p.i.) in SIVmac239-infected but not in Δ5G-infected or uninfected animals (Fig. 1C and D). These findings were consistent with values from whole-blood analysis (Fig. 1E and F). Notably, these differences were not secondary to differences in the expression of CCR5 by the CXCR3-expressing CD4$^+$ T cells since the level of CCR5-expressing cells within this subset was minimal (Fig. 1G). These data were consistent with the finding that the peak expression of cytokines and chemokines occurs prior to peak viremia in acute HIV infection (15), suggesting that these chemokines may influence the trafficking of the CXCR3$^+$ T cells from the blood to the tissues, including the SLOs, where the relevant chemokines are extensively expressed following SIVmac239 infection.

Transcriptome analyses demonstrated abundant expression of interferon (IFN)-stimulated genes (ISGs), antiviral factors, and pattern recognition receptor (PRRs), illustrating the occurrence of innate immune responses against SIVmac239 and Δ5G. Next, we performed transcriptome analyses using PBMCs collected from the infected animals at 7 days p.i., corresponding to approximately 3 to 5 days before peak viremia was achieved (Fig. 2A), as shown in previous reports (1, 13). Among the genes analyzed with a total of 44,000 probes, those corresponding to 4,256 probes showed a 2-fold change (>2 or <0.5) in expression between SIVmac239-infected and uninfected animals, Δ5G-infected and uninfected animals, or Δ5G- and SIVmac239-infected animals. Hierarchical clustering analyses identified six groups (G1 to G6), among which SIVmac239 infection predominantly upregulated the expression of most of genes clustered in G1, G3, and G5, whereas Δ5G infection upregulated the expression of most of genes in G1, G2, and G3 (Fig. 2B). These results indicated that the two viruses induced distinct host responses, which may be due to differences in the targeting of different subsets of CD4$^+$ T cells (1), as exemplified by the selective depletion of CXCR3$^+$ CCR5$^+$ CD4$^+$ T cells in SIVmac239- but not Δ5G-infected animals (Fig. 1G).

Several studies (16–19) have reported that SIV/HIV infection elicits robust innate immune responses highlighted by the expression of a number of genes, including IFN-stimulated genes (ISGs) and antiviral host factors that are triggered by pattern recognition receptors (PRRs) sensing viral and cellular components initiated during the early stage of infection. Therefore, we analyzed the expression of these genes and compared expression levels obtained during acute infection in SIVmac239- and Δ5G-infected animals (Fig. 2C and D; Tables 1 and 2). A number of ISGs were upregulated in PBMC samples obtained on day 7 p.i. from both SIVmac239- and Δ5G-infected animals (Fig. 2C). However, as shown in Table 1, the levels of expression of approximately 75% (17/23) of genes were 1.4- to 3.6-fold (mean, 2.4-fold) higher in PBMCs from SIVmac239-infected animals than in those from Δ5G-infected animals. Overall, the differences were consistent with the difference in levels of the expression of IFN-β1 (Table 1). This difference may be explained by the different levels of viral replication between the two viruses at 7 days p.i. (Fig. 2A). Thus, the innate antiviral responses associated with these genes may not be primarily directed at the live-attenuated properties of Δ5G, such as containment of viremia following primary infection in Δ5G- but not SIVmac239-infected animals, as previously reported (11).

Next, we examined the expression levels of genes that have been previously documented as naturally occurring antiretroviral host factors (20). As shown in Table 2 and Fig. 2D, the differences in expression levels of APOBEC3s, TRIMs, and BST2 between the two groups were less than 2-fold. Notably, the genes that distinguish the responses to acute infection with Δ5G from those with SIVmac239 exhibit inherent differences in the sensing of viral nucleic acids. Thus, while Toll-like receptor 7 (TLR7) senses viral RNA via the endosomal pathways (21, 22), DDX58/RIG-I and IFIHI1/MDA5 sense viral RNA in the cytosol of the cells (20). Expression levels of these genes were 2- to 3-fold higher in SIVmac239-infected animals than in Δ5G-infected animals, similar to the differences in the expression levels of ISGs (Tables 1 and 2).

Taken together, these results indicated that innate responses mediated by ISGs, antiretroviral host factors, and sensing viral nucleic acids occurred similarly during early acute infection in SIVmac239- and Δ5G-infected animals.
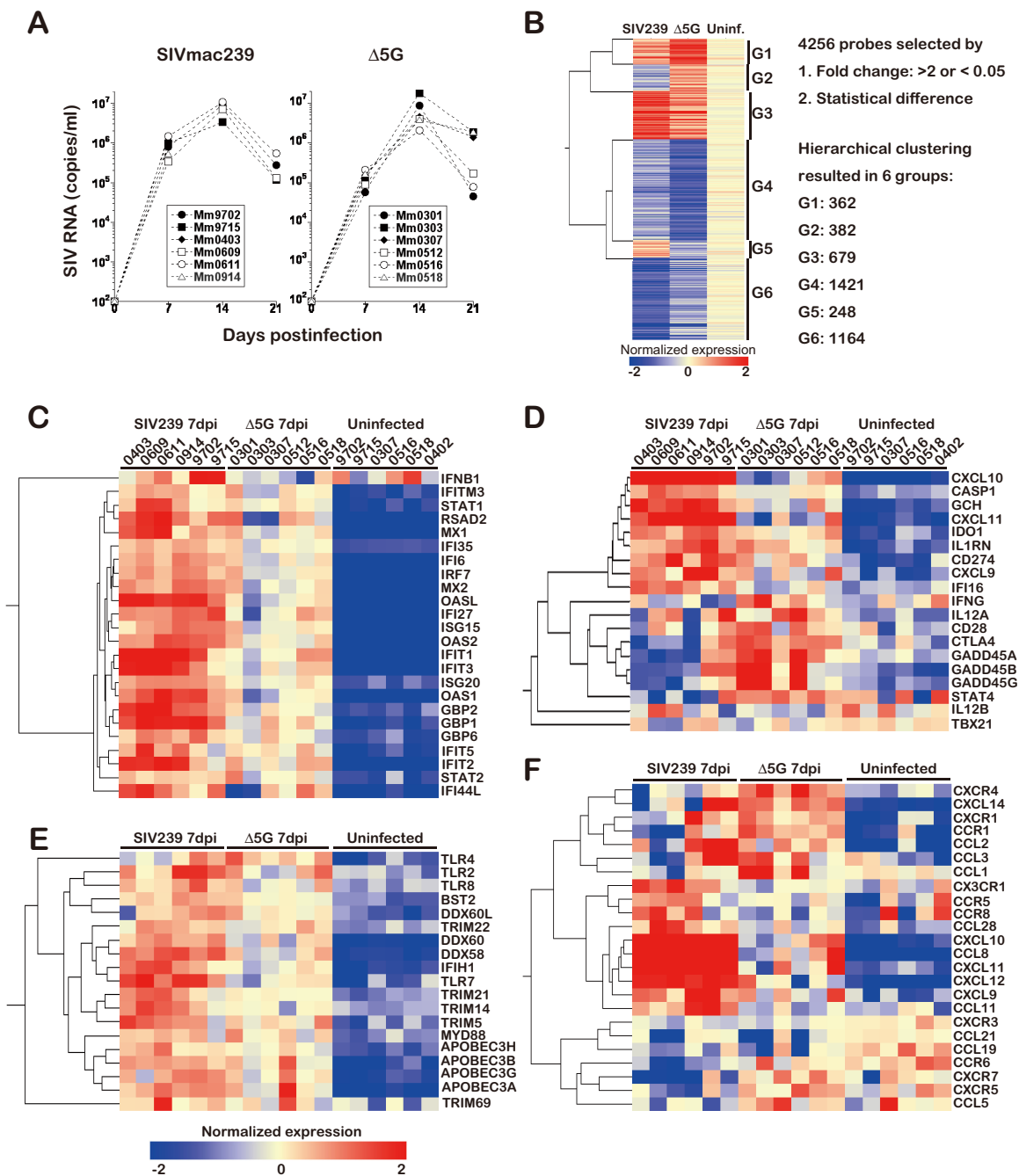
FIG 2 Expression of genes involved in type I interferon and innate antiviral responses, Th1-polarized inflammatory responses, and chemotaxis of immune cells. (A) SIV replication in the SIVmac239- and Δ5G-infected animals. (B) RNAs from the PBMCs of the SIV-infected and the uninfected animals ($n = 6$ each) were subjected to a rhesus macaque microarray (44,000 probes, version 2; Agilent Technologies). A total of 4,256 probes had significant differences (fold change of >2 or <0.5; statistical significance at a P value of <0.05) between two of three groups (SIVmac239- and Δ5G-infected and uninfected animals) and were clustered into six groups (G1 to G6). The heat maps show relative levels of gene expression normalized to the mean expression level of the controls (uninfected animals). The selected probes were sorted by the following gene functions: representative interferon-stimulated genes (ISGs) (C), genes related to innate responses and antiviral functions (D), genes related to T cell activation and Th1 differentiation (E), and chemokine-related genes (F). The heat maps show relative levels of gene expression in each animal normalized to the median expression level of all samples. Results were generated by hierarchical clustering analyses using the Subio Platform (Subio). dpi, days postinfection.

Th1-polarized responses and Th1 differentiation account for the differences in the outcomes of SIVmac239 and Δ5G SIV infections. Innate immune responses that are mediated through PRRs consist of antimicrobial responses, including the activation of proinflammatory genes (23). Depending on the type of microbes, the inflammatory

TABLE 1 Interferon-stimulated genes

Gene[a]	Relative expression in:					
	SIVmac239-infected vs Δ5G-infected animals		SIVmac239-infected vs uninfected animals		Δ5G-infected vs uninfected animals	
	Fold change[b]	P value	Fold change	P value	Fold change	P value
IFNB1	2.84	2.26E−02				
IFITM3			4.46	3.13E−06	3.38	1.06E−04
STAT1			5.65	2.64E−05	3.66	2.38E−06
RSAD2	2.82	2.23E−02	69.07	1.71E−07	24.52	1.39E−05
MX1	2.00	1.57E−02	18.90	4.14E−07	9.47	2.84E−07
IFI35	1.42	4.15E−03	3.55	9.39E−10	2.50	5.44E−07
IFI6	1.64	2.34E−03	24.73	5.20E−09	15.07	6.37E−08
IRF7	1.58	5.27E−03	12.59	1.73E−08	7.96	3.43E−07
MX2	1.84	3.20E−03	9.37	2.34E−09	5.10	1.17E−06
OASL	3.58	1.97E−05	22.52	1.78E−09	6.30	1.76E−06
IFI27	2.16	7.67E−03	33.07	3.36E−06	15.33	8.00E−05
ISG15	1.72	5.97E−03	47.91	2.81E−09	27.84	1.28E−08
OAS2	2.03	2.85E−04	10.79	8.13E−10	5.31	3.74E−08
IFIT1	3.25	2.89E−03	47.55	5.47E−06	14.61	4.22E−05
IFIT3	2.77	4.39E−03	35.64	3.44E−06	12.85	1.41E−05
ISG20	1.73	6.55E−05	4.07	4.70E−08	2.35	1.45E−05
OAS1	2.88	6.31E−04	43.29	4.48E−09	15.03	3.08E−07
GBP2	2.88	1.42E−04	6.94	9.79E−07	2.41	9.13E−05
GBP1	3.13	3.46E−05	13.84	3.78E−07	4.42	5.40E−05
GBP6			4.26	3.47E−06	2.57	1.24E−04
IFIT5			5.66	7.60E−05	4.09	8.76E−06
IFIT2	1.98	3.67E−02	20.93	2.37E−06	10.56	1.41E−06
STAT2			3.38	1.20E−05	2.78	8.45E−04
IFI44L	2.45	4.62E−02	28.05	3.26E−05	11.46	1.41E−03
Avg	2.35		20.70		9.11	

[a]All genes with the exception of IFNB1 belonged to group 3 as determined by hierarchical clustering analyses of transcriptome analysis data (Fig. 2B). IFNB1 belonged to group 5.
[b]Fold changes between two groups with statistically significant differences ($P < 0.05$) are shown.

responses trigger Th1 cell activation, which promotes adaptive immune responses (23, 24). In fact, as shown in a previous report (16), the expression of genes related to inflammatory and Th1 responses was associated with pathogenic rather than non-pathogenic SIV infection during the early stages. Thus, we next compared the expression levels of genes that were likely to be involved in the inflammatory responses and in T cell activation between SIVmac239- and Δ5G-infected animals. Genes involved in inflammasome activation include CASP1 and cytosolic and DNA sensor IFI16 (25). Interestingly, these genes were significantly activated but only in PBMCs from SIVmac239-infected animals (Fig. 2E; Table 3). Moreover, the degree of T cell activation reflected by the expression levels of GCH1 in PBMCs from SIVmac239-infected animals was 3.2-fold higher than those from Δ5G-infected animals. The expression of genes involved in general T cell activation was also evident, but the differences in expression levels were modest and not significant, as exemplified by the levels of expression of CD274, IDO1, and IL1RN. Nevertheless, differences in the expression levels of these genes were mostly similar to those observed for ISGs, antiretroviral host factors, and nucleic acid sensors (Tables 1 to 3). However, there was a more pronounced and significant difference in the expression levels of the genes associated with Th1 cell activation. Indeed, among the chemokines involved in the chemoattraction of CXCR3^{+} T cells, the expression levels of CXCL10 and CXCL11 were exceptionally high (10.3- and 7.1-fold, respectively) in PBMCs from SIVmac239-infected animals compared with those in PBMCs from Δ5G-infected animals (Table 3). These chemokines have previously been shown to play a critical role in the activation of CXCR3^{+} T cells in SLOs (26–28) and therefore may contribute to the increased frequencies of infected CD4^{+} T cells in SLOs in SIVmac239-infected animals.

In addition to the above-described increases in chemokine gene expression in PBMCs from SIVmac239-infected animals, significant upregulation was also observed

TABLE 2 Pattern recognition receptors and antiviral factors

	Relative expression in:					
	SIVmac239-infected vs Δ5G-infected animals		SIVmac239-infected vs uninfected animals		Δ5G-infected vs uninfected animals	
Gene[a]	Fold change[b]	P value	Fold change	P value	Fold change	P value
TLR4			2.79	2.00E−03	3.78	1.23E−04
TLR2			3.02	8.86E−04		
TLR8			2.25	5.33E−04		
BST2	1.33	9.49E−03	2.86	3.13E−06	2.14	1.97E−05
DDX60L			2.93	2.22E−03	2.70	7.22E−05
TRIM22			2.27	1.09E−04		
DDX60	1.71	1.01E−02	9.05	1.53E−07	5.31	1.55E−05
DDX58	2.23	5.01E−04	7.80	3.87E−10	3.50	6.24E−06
IFIH1	1.99	4.13E−03	6.12	1.45E−06	3.08	3.72E−06
TLR7	3.34	3.99E−04	7.40	6.13E−05	2.22	1.63E−02
TRIM21	1.57	2.67E−02	3.01	1.71E−04		
TRIM14	1.93	7.59E−03	2.88	1.36E−04		
TRIM5			3.60	4.72E−04	2.44	1.05E−03
MYD88			2.33	2.80E−04	2.18	1.22E−03
APOBEC3H	1.36	3.74E−02	3.32	4.13E−06	2.44	5.26E−06
APOBEC3B			5.61	7.51E−07	4.29	8.11E−05
APOBEC3G			4.86	1.10E−05	3.73	2.02E−05
APOBEC3A			17.03	1.85E−06	12.67	4.02E−05
TRIM69			2.06	2.06E−02		
Avg	1.93		4.80		3.88	

[a]All genes belonged to group 3 as determined from hierarchical clustering analyses of transcriptome analysis data (Fig. 2B).
[b]Fold changes between two groups with statistically significant differences ($P < 0.05$) are shown.

for GADD45A, GADD45B, GADD45G, and STAT4 (Fig. 2E and Table 3). These genes might be involved in the downregulation of immune responses in Δ5G-infected animals but not in SIVmac239-infected animals. GADD45 proteins have been reported to be involved in the differentiation and/or function of Th1 cells (29); GADD45A functions as a negative regulator of activation-induced T cell proliferation (30), whereas GADD45B and GADD45G are required for IFN-γ production by Th1 cells (21, 22, 31–33). STAT4 is required for interleukin-12 (IL-12)-dependent differentiation of Th1 cells (34). Indeed, the levels of IFN-γ expression were significantly higher in cells from Δ5G-infected animals than those from SIVmac239-infected animals (Table 3). These data implied that there were significant differences in the expression levels of genes involved in the differentiation and regulation of Th1 cell activation between Δ5G- and SIVmac239-infected animals.

Differential expression levels of select chemokine/chemokine receptor genes distinguished SIVmac239 from Δ5G infection. Chemokines play important roles in immune responses by directing the migration of select immune cells expressing the corresponding receptors to inflammatory effector sites, inductive tissues for initiating adaptive immune response, and/or residential tissues for homeostatic regulation (35). Interestingly, the expression levels of the CXCR3 ligand genes, including CXCL10 and CXCL11, were markedly higher in SIVmac239-infected than in Δ5G-infected animals (Table 3). We reasoned that these differences could account for the preferential infection of CD4$^+$ T cells in SLOs of SIVmac239-infected animals but not Δ5G-infected animals.

These findings prompted us to examine the expression levels of some additional chemokine and chemokine receptor genes in PBMCs from SIVmac239- and Δ5G-infected animals in greater detail (Fig. 2F and Table 4). Phylogenetic tree analyses were utilized to group the chemokines and chemokine receptors into three clusters (Fig. 2F). The genes clustered in the bottom rows of Fig. 2F were genes whose expression levels were lower in SIVmac239-infected animals than in uninfected animals and included genes encoding CCR6, CXCR7, CXCR5, and CCL5 (Table 4). The genes clustered in the upper rows were expressed at higher levels in PBMCs from Δ5G-infected animals than

TABLE 3 T cell activation and Th1 differentiation genes

Group and/ or gene[a]	Relative expression in:					
	SIVmac239-infected vs Δ5G-infected animals		SIVmac239-infected vs uninfected animals		Δ5G-infected vs uninfected animals	
	Fold change[b]	P value	Fold change	P value	Fold change	P value
G3						
CXCL10	10.26	3.45E−05	50.60	4.91E−08	4.93	8.23E−04
CASP1	1.77	9.64E−04	2.96	2.00E−05		
GCH1	3.17	8.40E−04	8.99	6.92E−07	2.84	4.15E−04
CXCL11	7.05	6.29E−04	17.30	1.95E−07	2.45	3.89E−02
IDO1			4.46	2.40E−05	2.83	4.11E−04
CD274	2.04	1.51E−02	6.14	2.00E−04	3.00	4.18E−03
IL1RN			5.15	2.49E−05	3.53	8.28E−05
CXCL9			6.34	2.01E−03	2.77	2.30E−02
IFI16	2.25	9.05E−04	2.78	5.12E−05		
Avg	4.42		11.68		3.19	
G2						
IFNG	0.46	2.70E−02				
IL12A	(0.74)		(2.05)		2.78	3.26E−03
CD28					2.07	3.73E−02
CTLA4	0.40	7.84E−03			2.42	1.41E−03
GADD45A	0.26	7.79E−03			2.87	1.78E−03
GADD45B					6.32	7.39E−03
GADD45G	0.16	1.96E−02			6.49	8.93E−03
STAT4	0.29	1.17E−02				
Avg	0.31				3.82	
IL12B	(1.34)		(0.87)		(0.65)	
TBX21	(0.97)		(0.76)		(0.78)	

[a]Groups were determined from hierarchical clustering analyses of transcriptome analysis data (Fig. 2B).
[b]Fold changes between two groups with statistically significant differences ($P < 0.05$) are shown (values shown in parentheses are not significantly different).

in uninfected animals and included genes encoding CXCR4, CXCL14, CXCR1, CCR1, CCL2, and CCL3. In contrast, genes clustered in the middle rows of Fig. 2F included genes encoding CXCL10 and CXCL11 (predominantly associated with a Th1 response) that were expressed at higher levels in PBMCs from SIVmac239-infected animals than in those from Δ5G-infected and uninfected animals (Table 4). Notably, the gene encoding CCL8 was expressed at a level 100-fold higher in PBMCs from SIVmac239-infected animals than in PBMCs from the uninfected animals. In addition, the expression levels of genes encoding chemokines (CXCL12, CXCL9, CCL11, and CCL28) and chemokine receptors (CCR8 and CX3CR1) were expressed at significantly higher levels in PBMCs from SIVmac239-infected animals than in those from Δ5G-infected animals. Since CCL8 functions as a chemokine for $CCR5^+$ cells, the higher expression levels of CXCL10, CXCL11, and CCL8 in SIVmac239-infected animals than in Δ5G-infected animals may be involved in the enhanced trafficking of CXCR3- and CCR5-expressing cells, such as $CCR5^+$ $CXCR3^+$ $CD4^+$ T cells, to tissues where these chemokines are expressed, such as the SLOs. In addition, we also noted upregulation in the expression of CX3CR1 in SIVmac239-infected animals. Since CX3CR1 is expressed by $CD16^+$ monocytes (36), we hypothesized that this cell lineage may have an important role during the early stages of primary infection, as outlined in studies of the pathogenesis of HIV/SIV infection (37).

SIVmac239 infection elicited robust CXCL10 expression. Transcriptome analyses revealed that CXCL10, CXCL11, and CCL8 mRNAs were markedly upregulated in PBMCs from SIVmac239-infected animals compared with levels in PBMCs from Δ5G-infected animals at 7 days p.i. (Fig. 2 and Table 4). Thus, we validated and compared mRNA levels of the CXCR3 chemokines and CCL8 using quantitative reverse transcription-PCR (qRT-PCR). Consistent with the microarray results, the mRNA levels of these chemokines in PBMCs from SIVmac239-infected animals were clearly different from those from

**TABLE 4** Chemokines and chemokine receptors

| Gene subset and name[a] | Group[b] | Relative expression in: | | | | | |
| | | SIVmac239-infected vs Δ5G-infected animals | | SIVmac239-infected vs uninfected animals | | Δ5G-infected vs uninfected animals | |
		Fold change[c]	P value	Fold change	P value	Fold change	P value
Genes differentially expressed in Δ5G-infected animals vs controls							
CXCR4	G2	0.32	6.54E−03			3.32	1.93E−04
CXCL14	G2			4.56	4.42E−02	6.65	3.26E−08
CXCR1	G2			3.17	1.55E−02	3.93	1.03E−03
CCR1	G2	0.34	2.01E−02			7.62	2.45E−03
CCL2	G3			28.03	2.55E−03	12.93	7.48E−04
CCL3	G2					2.63	4.69E−02
CCL1	G2	0.14	4.05E−02				
Avg						6.18	
Genes differentially expressed in Δ5G-infected animals vs SIVmac239-infected animals							
CX3CR1	G3	2.39	3.32E−03	2.34	1.15E−02		
CCR5		(1.50)		(2.16)		(1.44)	
CCR8	G2	2.30	3.31E−02				
CCL28	G2	1.99	2.20E−02	2.98	2.45E−03		
CXCL10	G3	10.26	3.45E−05	50.60	4.91E−08	4.93	8.23E−04
CCL8	G3	7.93	5.13E−04	166.41	3.56E−07	20.99	6.19E−05
CXCL11	G3	7.05	6.29E−04	17.30	1.95E−07	2.45	3.89E−02
CXCL12	G3	4.64	7.31E−04	25.88	2.06E−08	5.57	4.73E−04
CXCL9	G3			6.34	2.01E−03	2.77	2.30E−02
CCL11	G3	3.39	9.19E−03	3.49	9.53E−03		
Avg		4.99		34.42		7.34	
Genes differentially expressed in SIVmac239-infected animals vs controls							
CXCR3		(1.10)		(1.46)		(1.32)	
CCL21	G2					0.45	4.51E−02
CCL19	G2			0.49	6.45E−03	0.39	3.26E−02
CCR6	G2	0.41	1.85E−02	0.31	3.13E−03		
CXCR7	G2	0.24	1.93E−03				
CXCR5	G2	0.42	9.54E−03				
CCL5	G2	0.48	1.91E−02				
Avg		0.39					

[a]Genes are grouped according to the three clusters shown in Fig. 2F (see text).
[b]Groups were determined from hierarchical clustering analyses of transcriptome analysis data (Fig. 2B).
[c]Fold changes between two groups with statistically significant differences ($P < 0.05$) are shown (values shown in parentheses are not significantly different).

uninfected and Δ5G-infected animals (Fig. 3A). While CXCL9 mRNA levels in PBMCs from SIVmac239-infected animals were slightly higher than those in PBMCs from uninfected animals, significant increases in CXCL10, CXCL11, and CCL8 mRNAs (32-, 15-, and 43-fold, respectively) were observed in PBMCs from SIVmac239-infected animals compared with levels in PBMCs from uninfected animals. Moreover, although the levels of CXCL10, CXCL11, and CCL8 mRNAs in PBMCs from the Δ5G-infected animals were also higher than those in PBMCs from uninfected animals, the relative levels were significantly lower (2.8-, 1.2-, and 6.9-fold, respectively). Overall, the fold change results determined by the qRT-PCR were well correlated with those determined by the microarray analysis ($P = 0.0006$, Spearman $r = 0.781$) (data not shown). More importantly, the differences in mRNA levels among these chemokines were evident (Fig. 3A). Thus, the median level of CXCL10 mRNA in SIVmac239-infected animals was 1 to 2 logs (20-, 15-, and 70-fold) higher than the levels of CXCL9, CXCL11, and CCL8, respectively, indicating that CXCL10, a major CXCR3 chemokine, could be responsible for the depletion of CXCR3^{+} T cells in the blood at 7 days p.i. (Fig. 1).
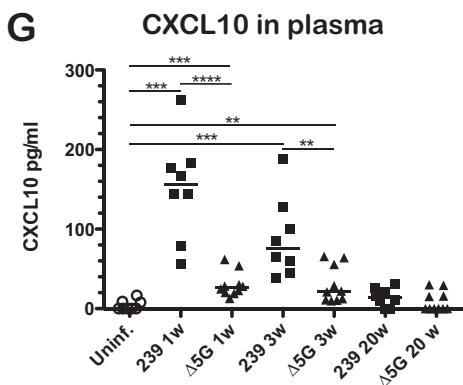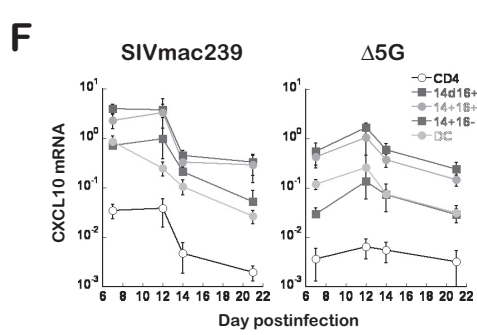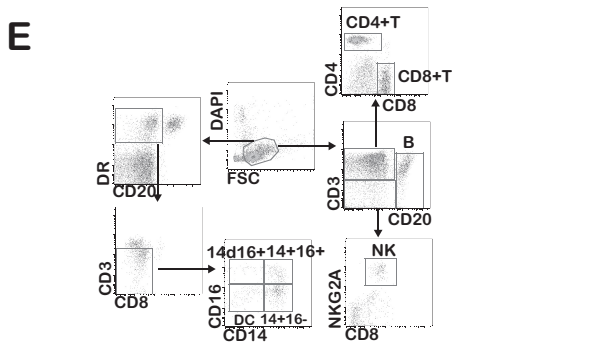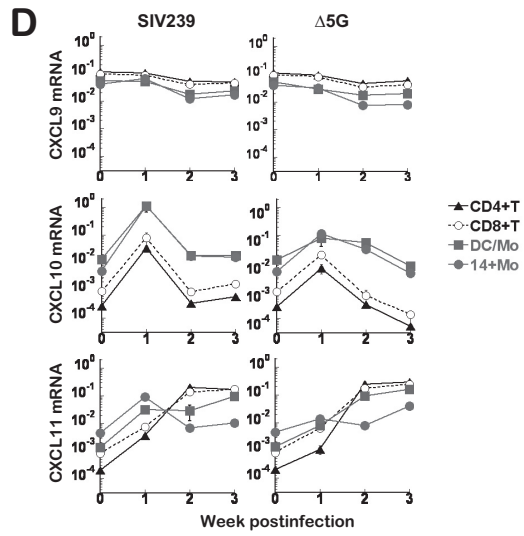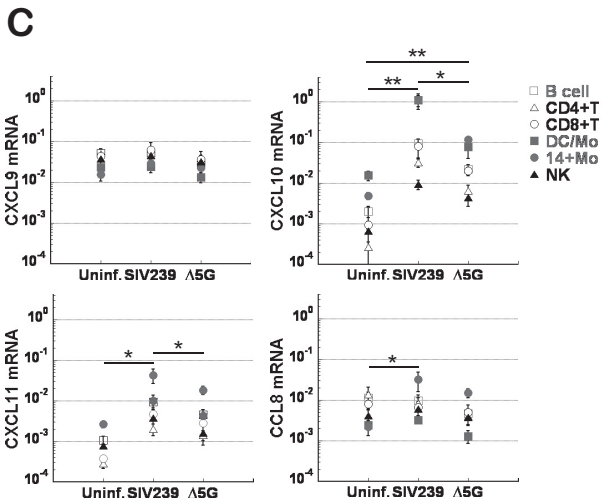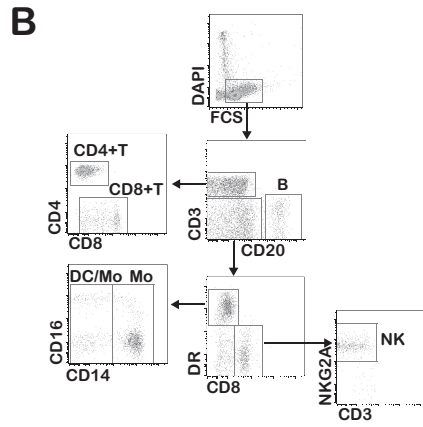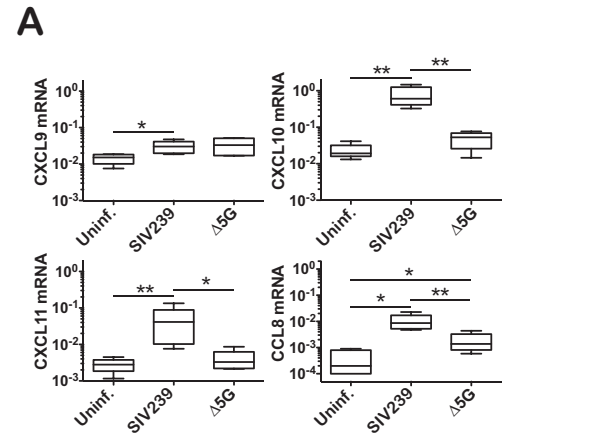
To trace the source of the differences in expression of CCL8 and CXCR3 chemokines, CXCL9, CXCL10, and CXCL11, we utilized flow cytometry-assisted cell sorting for the isolation of specific immune cells from PBMCs collected at 7 days p.i. (Fig. 3B) and examined expression of these chemokines by qRT-PCR. As shown in Fig. 3C, CXCL9 mRNA levels were comparable among subsets, but CXCL10 abundance was markedly variable. For example, while the cell fraction containing $CD14^{dim}$ (weakly positive) $CD16^+$ monocytes and $CD14^- CD16^+$ dendritic cells (DCs) (Fig. 3B) expressed the highest levels of CXCL10 mRNA in all animals, expression levels were 1 log (9.4- and 14.2-fold) and 2 logs (220- and 71-fold) higher in the animals infected with SIVmac239 than in Δ5G-infected and uninfected animals, respectively. Similarly, expression levels of CXCL11 in most immune cells and of CCL8 in $CD14^+$ monocytes were significantly variable but were generally more than 1 log lower than those of CXCL10 (Fig. 3C). In addition, expression levels of CXCR3 chemokines in $CD14^+$ monocytes, DCs/monocytes, $CD4^+$ T cells, and $CD8^+$ T cells exhibited different trends from 0 to 3 weeks postinfection (p.i.) (Fig. 3D). In particular, CXCL10 expression resembled plasma viral load (1), indicating that CXCL10 impacts SIV infection, or vice versa.

Since CXCL10 was most abundantly expressed in fractions containing monocytes, we further examined expression in the monocyte subsets, that is, $CD14^+ CD16^-$, $CD14^+ CD16^+$, and $CD14^{dim} CD16^+$ cells, as well as in $CD14^- CD16^-$ DCs. For comparison, expression was also assessed in $CD4^+$ T cells. These subsets were isolated from the PBMCs of SIVmac239- and Δ5G-infected animals between days 7 and 21 p.i. (Fig. 3E). Results show that in both groups, expression levels were highest in $CD14^{dim} CD16^+$ and $CD14^+ CD16^+$ monocytes, followed by those in $CD14^+ CD16^-$ monocytes and DCs (Fig. 3F). However, mean expression levels in all monocyte subsets and $CD4^+$ T cells were 12- and 5-fold higher, respectively, at 7 and 12 days p.i. in animals infected with SIVmac239 than in Δ5G-infected animals.

Collectively, the data suggest that CXCL10 is the major CXCR3 chemokine differentially and abundantly expressed at 7 days p.i. with SIVmac239, mostly by $CD14^+ CD16^+$ and $CD14^{dim} CD16^+$ monocytes. Correlations between expression levels of CXCL10 and viral loads suggest a critical role of the $CD16^+$ monocyte subsets in SIV infection.

To validate these results, we measured CXCL10 in plasma. CXCL10 levels at 1 week p.i. were highest in SIVmac239-infected animals although levels decreased at 3 weeks p.i. but nevertheless remained detectable at 20 weeks p.i., with medians of 156, 75.0, and 13.5 pg/ml, respectively (Fig. 3G). In contrast, CXCL10 levels at 1 and 3 weeks p.i. were significantly lower at 12.9 and 9.8 pg/ml, respectively, in Δ5G-infected animals. At 20 weeks p.i., CXCL10 levels had returned to baseline and were undetectable in most Δ5G-infected animals. These results indicate that plasma CXCL10 levels at 1 week p.i. were 10-fold higher in SIVmac239-infected animals, in line with mRNA measurements.

SIVmac239 infection elicited distinct increases of $CD14^+ CD16^+$ monocytes that express highest levels of CXCL10. Monocytes, DCs, and macrophages play pivotal roles in innate immunity by their ability to sense a variety of microbes and exert diverse antimicrobial and inflammatory responses (36, 38). As noted, $CD16^+$ monocyte subsets were the key producers of CXCL10 early in primary infection. Accordingly, we examined the abundance of monocyte subsets in PBMCs during primary infection. As shown in Fig. 4A, the frequencies of $CD14^+ CD16^+$ subsets in monocytes were

FIG 3 Expression of CXCL9, CXCL10, CXCL11, and CCL8 in SIV-infected and uninfected animals. (A) CXCL9, CXCL10, CXCL11, and CCL8 mRNAs in PBMCs collected at 7 days p.i. Data (relative to GAPDH mRNA expression) are shown by box and whisker plots. (B) Gating strategy used in the experiments shown in panels C and D. PBMCs were sorted to isolate $CD4^+$ T, $CD8^+$ T, B, and NK cells, as well as $CD14^+$ monocytes, and $CD14^{dim}$ monocytes/DCs. (C) CXCL9, CXCL10, and CXCL11 mRNAs in $CD4^+$ T, $CD8^+$ T, B, NK cells, the $CD14^{dim}$ monocytes/DCs, and $CD14^+$ monocytes (14^+ Mo) in PBMCs at 7 days p.i. Data are means ± standard errors of the means. Statistically significant pairwise differences ($CD14^+$ monocytes) are marked. (D) CXCL9, CXCL10, and CXCL11 mRNAs in $CD4^+$ T, $CD8^+$ T, $CD14^{dim}$ monocytes/DCs, and $CD14^+$ monocytes in PBMCs at 0 to 3 weeks p.i. Data are means ± standard errors of the means. (E) Gating strategy used in the experiment shown in panel F. PBMCs were sorted to isolate $CD14^+ CD16^-$, $CD14^+ CD16^+$, and $CD14^{dim} CD16^+$ monocytes, as well as $CD14^{dim} CD16^-$ DCs and $CD4^+$ T cells. (F) CXCL10 mRNA in $CD14^{dim} CD16^+$ ($14d 16^+$), $CD14^+ CD16^+$, and $CD14^+ CD16^-$ monocytes, $CD14^- CD16^-$ DCs (DC), and $CD4^+$ T cells in PBMCs at 7 to 21 days p.i. Data are means ± standard errors of the means. (G) CXCL10 concentration in plasma at 1, 3, and 20 weeks p.i. Statistically significant pairwise differences are marked. *, $P < 0.05$; **, $0.01 < P < 0.05$; ***, $0.001 < P < 0.01$; ****, $P < 0.0001$; DC/Mo, fractions containing DCs and $CD14^{dim} CD16^+$ monocytes.
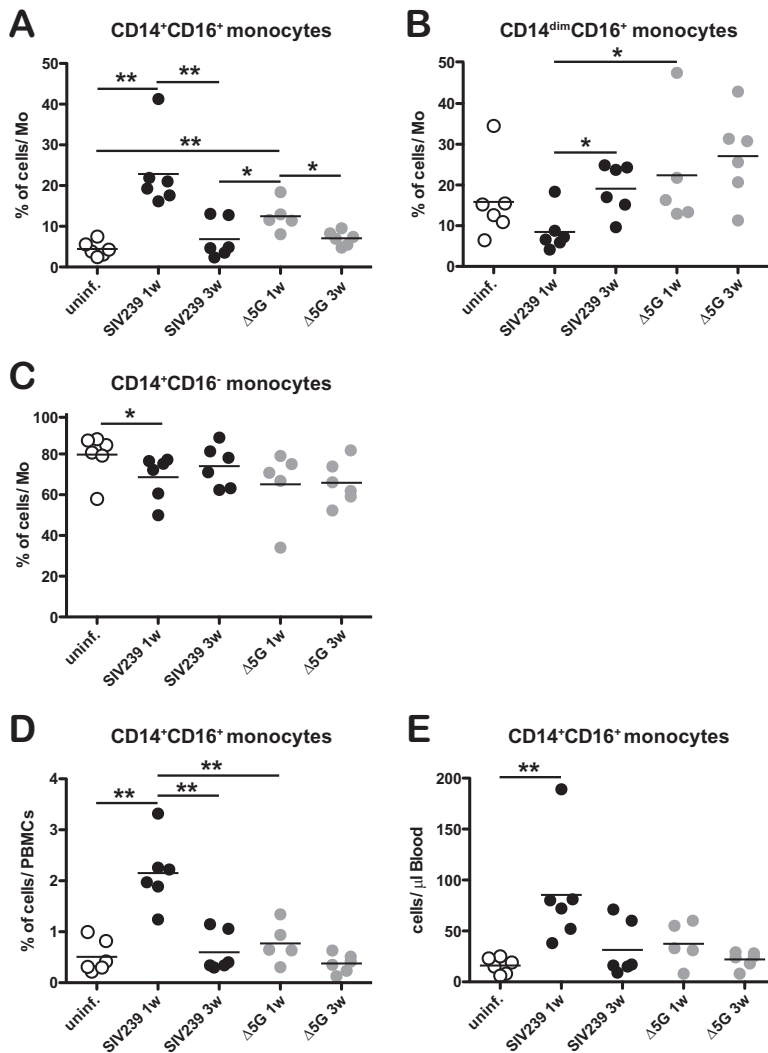
FIG 4 Frequencies of monocyte subsets in SIVmac239- and Δ5G-infected animals. CD14$^+$ CD16$^+$ (A), CD14^{dim} CD16$^+$ (B), and CD14$^+$ CD16$^-$ monocytes (C) populations are shown as percentages of total monocytes. CD14$^+$ CD16$^+$ monocytes are shown as a percentage of PBMCs (D) or as absolute numbers of cells per microliter of blood (E). Statistically significant pairwise differences are marked. *, $P < 0.05$; **, $0.01 < P < 0.05$.

significantly higher in SIVmac239-infected animals at 1 week p.i. although those decreased to baseline at 3 weeks p.i. Similar trends were observed in Δ5G-infected animals although the frequencies at 1 week p.i. were significantly lower than those in SIVmac239-infected animals.

Notably, changes in the CD14$^+$ CD16$^+$ subset appeared to drive the abundance of all other monocyte subsets in SIVmac239-infected animals. For instance, the frequencies of the CD14$^+$ CD16$^-$ subset at 1 week p.i. were lower than those in the uninfected animals (Fig. 4C), and the frequencies of the CD14^{dim}CD16$^+$ subset at 3 weeks p.i. were higher than those at 1 week p.i. (Fig. 4B). The decrease of the CD14$^+$ CD16$^+$ subset from 1 to 3 weeks p.i. was likely due to the differentiation of the monocyte subsets into the CD14^{dim} CD16$^+$ subset as previously reported (39). Collectively, these results indicate that the abundance of the CD14$^+$ CD16$^+$ subset increased 1 week after infection with SIVmac239 (Fig. 4D and E). The expression levels of CXCL10 coincided with this increase, implying that the CD14$^+$ CD16$^+$ subset is a principal source of the chemokine in SIV-infected animals.

CD14$^+$ macrophages express the highest levels of CXCL10 in SLOs. As CXCL10 was abundantly expressed in peripheral blood monocytes (Fig. 3) from SIVmac239-

infected animals, we also assessed CXCL10 expression in macrophages in the mesenteric and inguinal LNs and in the spleen at 9 and 12 days p.i. (1). For comparison, we also measured expression in DCs and in $CD4^+$ T, $CD8^+$ T, NK, and B cells from the same tissues (Fig. 5D). In the mesenteric LNs and spleen of infected animals, CXCL10 expression peaked at 9 days p.i. and at 12 and 9 days p.i. in inguinal LNs from SIVmac239- and Δ5G-infected animals, respectively. In addition, the highest levels were detected in macrophages and were 5- to 23-fold (mean, 9-fold) higher in SIVmac239-infected animals than in Δ5G-infected animals (Fig. 5A to C). Notably, $CD14^+$ macrophages expressed distinctly higher levels of CXCL10 than $CD14^-$ macrophages, indicating that the former were major producers. In spleen, monocyte-derived macrophages expressed the highest level of CXCL10. Intriguingly, expression levels of CXCL10 in $CD4^+$ T cells in SLOs were 2- to 5-fold higher at 9 days p.i. in SIVmac239-infected animals than in Δ5G-infected animals but 16- to 46-fold higher at 12 days. This result indicates an increase in activated $CD4^+$ T cells, likely due to the type I IFN response as reported previously (40), in the former, loss of the same cells in the latter, or both.

SIVmac239 infection significantly increases the abundance of $CD14^+$ macrophages in SLOs. To examine whether CXCL10 expression was correlated with the abundance of specific immune cells, we examined, by flow cytometry, frequencies of $CD4^+$ T, $CD8^+$ T, B, and NK cells and $CD14^+$ macrophages in SLOs at 9 to 12 days p.i. (Fig. 6E). Only $CD14^+$ macrophages were markedly more abundant in SIVmac239-infected animals than in Δ5G-infected and uninfected animals (Fig. 6A to C). In the spleen, B and $CD4^+$ T cells were significantly more and less abundant, respectively, in SIVmac239-infected animals than in uninfected animals. Since most spleen macrophages are derived from monocytes, $CD14^+$ $CD16^-$, $CD14^+$ $CD16^+$, $CD14^{dim}$ $CD16^+$, and $CD14^-$ $CD16^-$ subsets were also examined. As shown in Fig. 6D, frequencies of the $CD14^+$ subsets ($CD14^+$ $CD16^-$ and $CD14^+$ $CD16^+$ cells) were significantly higher in SIVmac239-infected than in uninfected animals. These results indicate that the increase of $CD14^+$ macrophages in SIVmac239-infected animals is associated with robust CXCL10 expression.

Infiltration of $MAC387^+$ macrophages into SLOs correlates with higher levels of CXCL10 expression in SIVmac239-infected animals. $CD14^+$ macrophages are considered to have migrated and differentiated from monocytes and thus have different properties and functions from tissue-resident macrophages (38). In particular, $MAC387^+$ macrophages were demonstrated as recently infiltrated to play key roles in inflammatory responses in SIV encephalitis (41). We previously reported that $MAC387^+$ macrophages accumulate in regions adjacent to high endothelial venules (HEVs) in the paracortex of LNs from SIVmac239-infected animals during primary infection (42). Hence, we investigated whether $MAC387^+$ macrophages infiltrating into and eliciting inflammatory responses in SLOs drive CXCL10 expression in SIVmac239-infected animals. In line with RNA levels (Fig. 5), we detected CXCL10 expression in $MAC387^+$ $CD11b^{++}$ cells, which correspond to $MAC387^+$ $CD14^+$ cells (Fig. 7A), but not in T, B (Fig. 7C), and NK cells (data not shown).

We found that frequencies of $MAC387^+$ $CD11b^{++}$ cells in the mesenteric LNs from uninfected, SIVmac239-infected (7 to 12 days p.i.), and Δ5G-infected (7 to 14 days p.i.) animals were 0.03 to 0.14 (percent in mononuclear cells; mean, 0.05), 0.60 to 1.29 (mean, 0.81), and 0.05 to 0.08 (mean, 0.06), respectively (Fig. 8A). Thus, the frequencies in SIVmac239-infected animals were 1 log higher than those in uninfected and Δ5G-infected animals, as was noted in the previously reported pathological results (42). Similarly, frequencies of the cells in the inguinal LNs were 0.08 to 0.21 (mean, 0.13), 0.48 to 1.88 (mean, 1.02), and 0.10 to 0.56 (mean, 0.30), respectively (Fig. 8B). Of note, the frequencies increased in SIVmac239-infected animals between 7 and 12 days p.i., which is also in line with the previously reported pathological results. In contrast, the frequencies in Δ5G-infected animals decreased between 9 and 12 to 14 days p.i.

In the spleen, frequencies of the cells were 0.86 to 1.13 (mean, 0.99), 1.78 to 10.6 (mean, 4.33), and 0.61 to 1.78 (mean, 1.28), respectively (Fig. 8C). As noted, monocytes
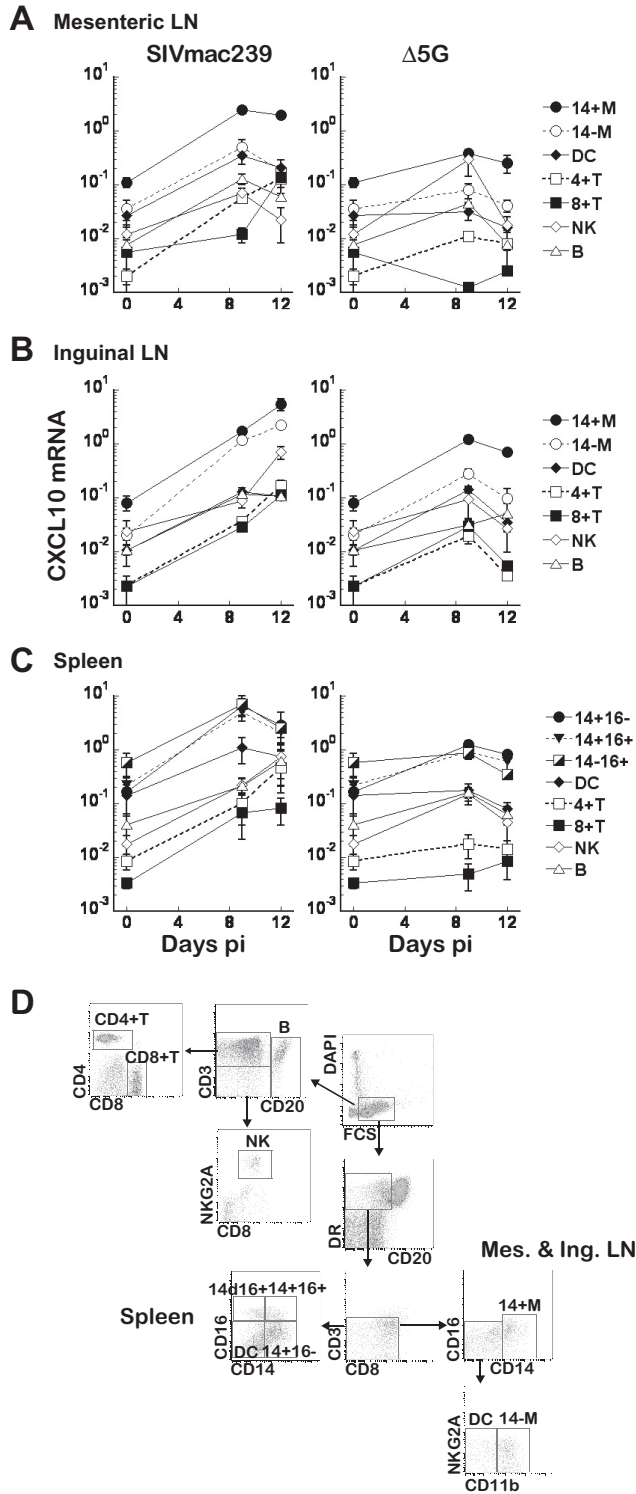
FIG 5 CXCL10 mRNA in SLOs. CXCL10 mRNAs in the mesenteric (A) and inguinal (B) LNs and spleen (C) are shown. Expression was analyzed in cell lineages isolated by flow cytometry (D) prior to (0 days) and 9 to 12 days p.i. In mesenteric LNs, lineages consisted of CD14$^+$ and CD14$^-$ macrophages (14$^+$ M and 14$^-$ M, respectively), as well as DCs, CD4$^+$ T (4$^+$ T), CD8$^+$ T (8$^+$ T), B, and NK cells. In inguinal LNs, CD14$^+$ and CD14$^-$ macrophages were analyzed along with DCs, CD4$^+$ T, and NK cells. In spleen, these cells consisted of CD14^{dim} CD16$^+$, CD14$^+$ CD16$^+$, and CD14$^+$ CD16$^-$ macrophages, as well as DC, CD4$^+$ T, B, and NK cells. Data are means $\pm$ standard errors of the means. (D) Gating strategy used. Immune cells isolated from mesenteric and inguinal LNs were sorted to isolate CD4$^+$ T, CD8$^+$ T, B, and NK cells, as well as CD14$^+$ and CD14$^-$ macrophages. Immune cells isolated from spleen were sorted to isolate CD4$^+$ T, CD8$^+$ T, B, and NK cells, as well as CD14^{dim} CD16$^-$ DCs and CD14$^+$ CD16$^-$, CD14$^+$ CD16$^+$, and CD14^{dim} CD16$^+$ macrophages.
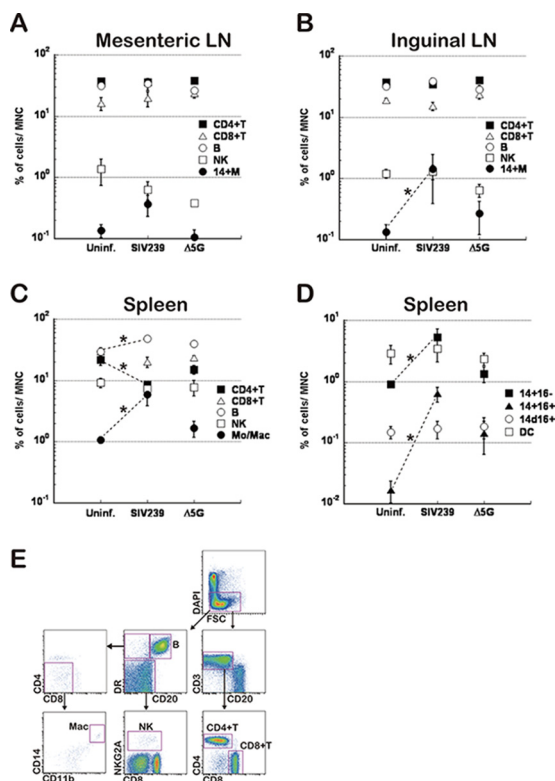
FIG 6 Frequencies of immune cells in SLOs. Frequencies of CD4$^+$ T, CD8$^+$ T, B, and NK cells in the mesenteric (A) and inguinal (B) LNs and spleen (C) and those of CD14^{dim} CD16$^+$ (14d 16$^+$), CD14$^+$ CD16$^+$, and CD14$^+$ CD16$^-$ macrophages and DCs in spleen (D) are shown. (E) Frequencies of immune cells were determined by flow cytometry at 9 to 12 days p.i. Statistically significant pairwise differences are marked. *, $P < 0.05$. MNC, mononuclear cell.

that express MAC387 tend to accumulate in the spleen, and, as a result, MAC387$^+$ CD11b^{++} cells are more abundant in this tissue than in the LNs. In any case, the MAC387$^+$ CD11b^{++} cells were significantly more abundant in SLOs in SIVmac239-infected animals than in uninfected and Δ5G-infected animals (Fig. 8, left panels). Similarly, frequencies of CXCL10$^+$ MAC387$^+$ CD11b$^+$ cells in SLOs were also significantly higher in SIVmac239-infected animals than in Δ5G-infected animals and uninfected animals (Fig. 8, right panels).

Collectively, these results indicate that distinctly higher expression levels of CXCL10 in SIVmac239-infected animals were associated with the increased abundance of MAC387$^+$ macrophages, suggesting that they have a role in the innate/inflammatory responses and the infection of CD4$^+$ T cells in SLOs.

DISCUSSION

The host immune system recognizes microbial infections and associated tissue damage by the innate immune cells, and that causes immune activation and inflammatory responses (23, 43). Whereas immune responses occur to remove the infected cells and to repair tissue damage, inflammatory responses, as described herein, play a key role in the pathogenesis of HIV infection, as reported previously (44). In contrast, infections with live-attenuated primate lentiviruses elicit lower inflammatory responses and levels of T cell activation than those with pathogenic SIV. We previously reported that infection with a ΔNef strain induced lower levels of MAC387$^+$ macrophages in paracortex of LNs during primary infection than SIVmac239 infection (42). Infection with SHIV89.6, a live-attenuated simian-human immunodeficiency virus (SHIV), decreased plasmacytoid DCs (pDCs), suppressed T cell activation, and increased regulatory T cells in rhesus macaques (45). Moreover, in natural hosts, such as African green monkey and
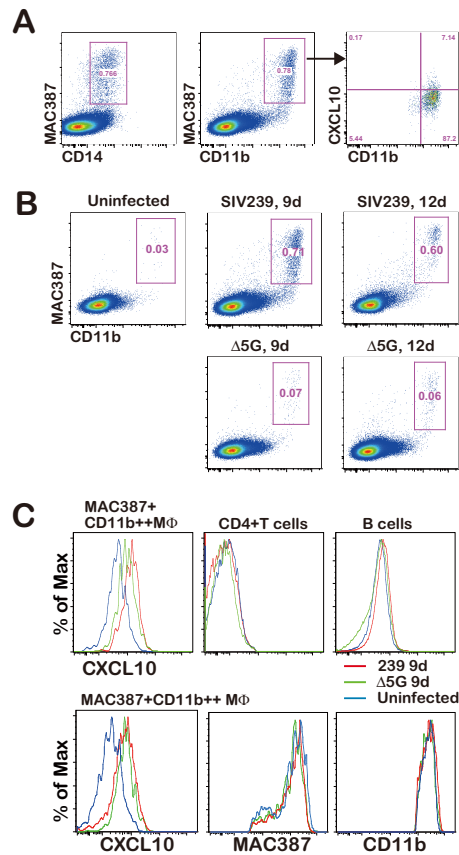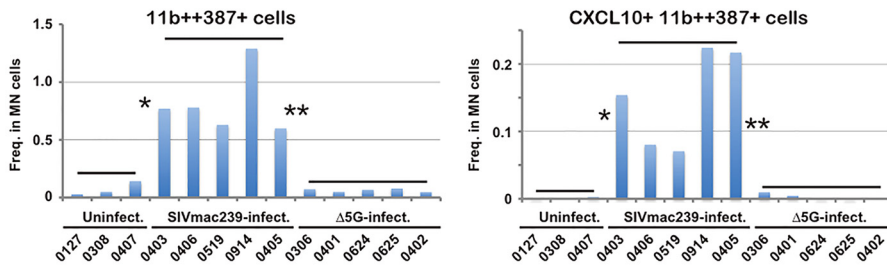
FIG 7 Induction of MAC387+ CD11b++ macrophages in mesenteric LNs of SIVmac239-infected animals. (A) MAC387+ CD11b++ macrophages are CD14+ and express CXCL10. (B) Frequencies of MAC387+ CD11b++ macrophages in mononuclear cells in Δ5G-infected animals were as low as those in uninfected animals but were markedly higher in SIVmac239-infected animals. (C) CXCL10 is distinctly expressed in MAC387+ CD11b++ macrophages but not in CD4+ T and B cells among SIVmac239- and Δ5G-infected and uninfected animals. Histograms show differential expression of CXCL10 but not MAC387 and CD11b in uninfected, SIVmac239-infected, and Δ5G-infected animals. d, days. The numbers in the boxes within the graphs in panels A and B are the frequencies (%) of MAC387+ CD11b++ macrophages in mononuclear cells.

sooty mangabey, the infection with SIVagm and SIVsm, respectively, elicits a robust but transient type I IFN-related innate response, resulting in a lack of immune activation, with few CCR5+ CD4+ T cells in SLOs (17, 18, 46). Importantly, whereas magnitudes of SIV infection in natural hosts are similarly high as those of pathogenic SIV infection in macaques, nevertheless, the infection does not cause pathogenic outcomes (47), implying that the sustained inflammatory response but not SIV infection is associated with the pathogenesis. Interestingly, monocytes and macrophages have been demonstrated to play key roles in the pathogenesis of HIV/SIV infection since they are involved in immune activation/inflammation in chronic infection (48, 49). The present study mostly supports these findings.

Studies of genome-wide transcriptomes revealed that infection with SIVmac239 elicits distinctly stronger inflammatory immune responses than infection with Δ5G. Such responses activate Th1 cells via robust expression of CXCR3 chemokines, especially CXCL10, the expression of which paralleled viral loads. We also found that CD14+ CD16+ monocytes in blood and MAC387+ macrophages in SLOs expressed the highest levels of CXCL10. Indeed, the abundance of MAC387+ macrophages infiltrated in SLOs was remarkably correlated with the magnitude of SIVmac239 infection (1). Collectively, these results illustrate the critical role of CD14+ CD16+ monocytes and MAC387+ macrophages in the innate inflammatory response to HIV/SIV (Fig. 9A). Unfortunately, such a response then triggers a vicious cycle that involves activation of CXCR3+ CD4+
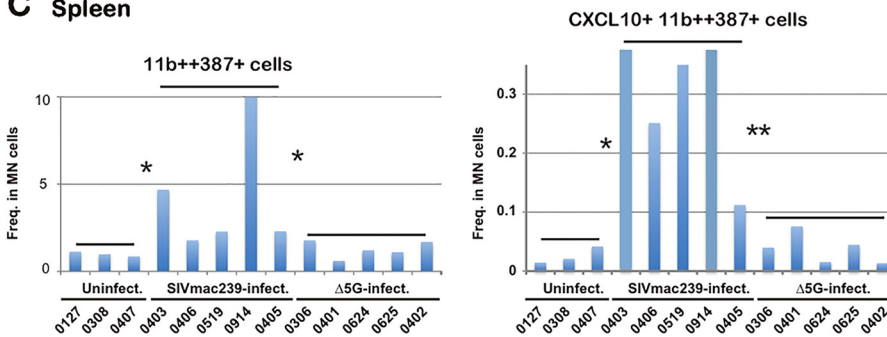
A Mesenteric LN

B Inguinal LN
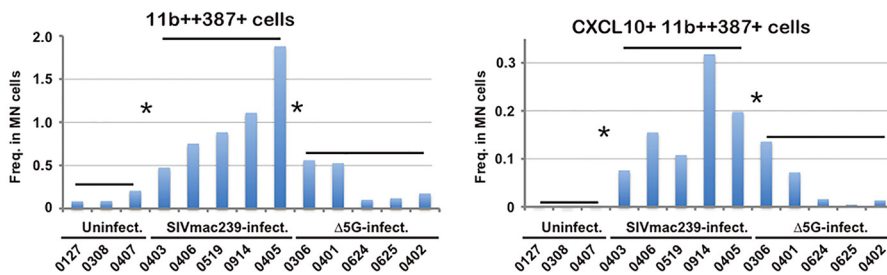
C Spleen

FIG 8 Distinctly high abundance of MAC387$^+$ CD11b^{++} macrophages correlates with SIVmac239 infection of Th1 cells in SLOs. Percent MAC387$^+$ CD11b^{++} macrophages (left) and CXCL10$^+$ cells (right) in mononuclear (MN) cells from mesenteric (A) and inguinal (B) LNs and in spleen (C) at 7 to 14 days p.i. with SIVmac239 and Δ5G. Statistically significant pairwise differences are marked. Uninfected animals include Mm0127, Mm0308, and Mm0407; SIVmac239-infected animals (days p.i.) include Mm0403 (7), Mm0406 (9), Mm0519 (9), Mm0914 (11), Mm0405 (12); Δ5G-infected animals include Mm0306 (9), Mm0401 (9), Mm0624 (12), Mm0625 (12), and Mm0402 (14).

T cells, infection of Th1 cells, and compromised adaptive immune responses, ultimately resulting in pathogenic and persistent infection.

CXCL10, a chemokine induced by proinflammatory stimuli, facilitated trafficking of effector Th1 cells to inflamed tissues (50, 51). Subsequently, CXCL10 was detected in inflamed SLOs, suggesting that the chemokine indeed activates and differentiates resting CD4$^+$ T cells into functional Th1 cells. DCs in a mouse model of liver granulomatous disease were also shown to express CXCL10 within 7 days after infection with *Propionibacterium acnes*, thereby recruiting proliferating Th1 cells to form clusters of IFN-γ-producing CD4$^+$ T cells (52). More recently, several studies reported a role for the CXCR3 and CXCR3 ligands (CXCL10 and CXCL9) for intralymphoid organ relocation of naive/resting CD4$^+$ T or CD8$^+$ T cells upon contact with antigen-loaded antigen-presenting cells and their subsequent differentiation into functional effector cells (26–28).

Peripheral blood monocytes consist of CD14$^+$ CD16$^-$ (>80%), CD14^{dim} CD16$^+$ (5 to 10%), and CD14$^+$ CD16$^+$ (<5%) cells. These subsets exert distinct functions and play important roles in the defense against microbial infections and sterile inflammations
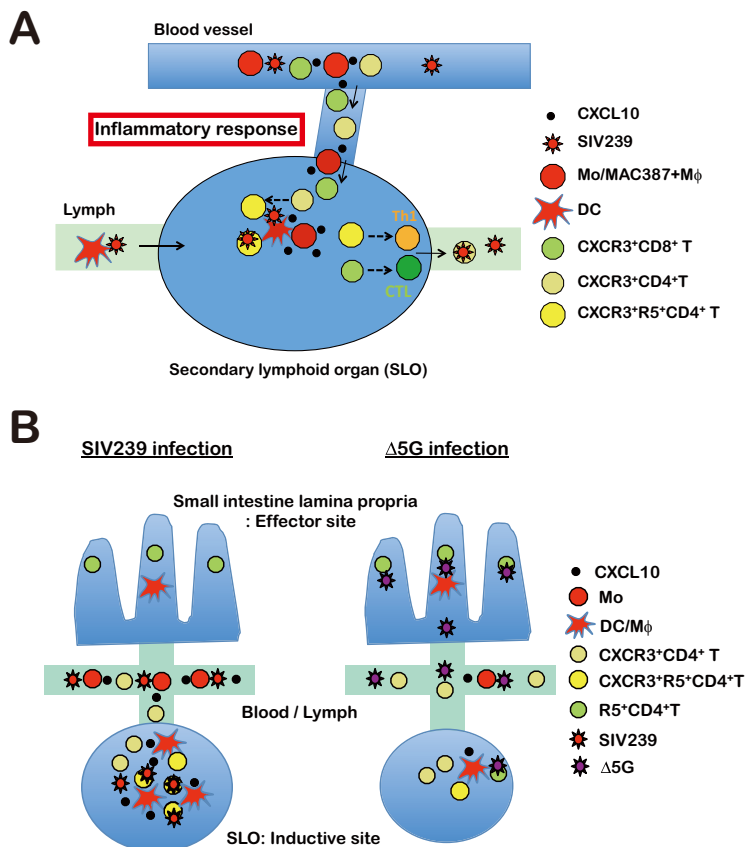
FIG 9 A working model for SIVmac239 targeting of CXCR3$^+$ CD4$^+$ T cells in SLOs. (A) T cells, B cells, and other immune cells in blood migrate to SLOs through HEVs and egress from the tissues by using chemokines, cell adhesion molecules, and other molecules. Upon SIV infection, monocytes are activated and express high levels of CXCL10 due to the inflammatory response and/or sensing SIV. These cells then migrate to the inflammatory tissues such as SLOs through HEVs where SIV infection has occurred. Since newly infiltrated monocyte-derived MAC387$^+$ macrophages (Mϕ) secrete inflammatory cytokines and chemokines such as CXCL10, CXCR3$^+$ T cells and other inflammatory cells accumulate at the inflammation sites, where SIVmac239 infects CXCR3$^+$ CCR5$^+$ CD4$^+$ T cells as previously reported (1). As a result, preferential infections of CCR5$^+$ CXCR3$^+$ CD4$^+$ T cells cause depletion of functional Th1 cells that are required for a cellular immune response to contain the infection. (B) Targeting of distinct CD4$^+$ T cell subsets by SIVmac239 and Δ5G. While SIVmac239 targets the CXCR3$^+$ CD4$^+$ T cells in SLOs, Δ5G primarily targets the CXCR3$^-$ CD4$^+$ T cells in the lamina propria of the small intestine, likely associated with potent adaptive immune responses elicited by high levels of infection in these tissues, as reported previously (1).

(36, 39). For example, CD14$^+$ CD16$^+$ monocytes, while a minor population at baseline, dramatically increase in abundance and acquire proinflammatory properties upon infection with HIV/SIV and a number of other microorganisms (53) and/or upon stimulation with other inflammatory agents (37). CD14$^+$ CD16$^+$ monocytes are associated with the pathogenic immune activation that shares mechanistic similarities with the studies reported here (54).

On the other hand, MAC387$^+$ macrophages have been demonstrated to infiltrate brain tissues, express CD14 and CD16 thereafter, and trigger SIV-associated encephalitis (41), suggesting a link between these macrophages and CD14$^+$ CD16$^+$ monocytes, as we observed in SLOs. In addition, lesions that form in SIV-associated encephalitis (41) are intriguingly similar to those observed near HEVs in the paracortex of LNs from SIVmac239-infected animals (42). Indeed, the former (41) consist of MAC387$^+$ macrophages, CD163$^+$ CD68$^+$ MAC387$^-$ perivascular macrophages, and CD68$^+$ HAM56$^+$ resident macrophages, while the latter (42) consist of MAC387$^+$ macrophages, CD68$^+$ HAM56$^+$ macrophages, plasmacytoid monocytes (pDCs), and activated T cells. Importantly, these cell clusters contained SIV-infected cells in both cases, suggesting that these cell clusters form niches where CD4$^+$ T cells are activated for productive SIV

infections under the inflammatory responses. Very few MAC387$^+$ macrophages were in SLOs from Δ5G-infected animals, which suggests that various live-attenuated SIVs and HIV controllers have similarly low levels of MAC387$^+$ macrophages in SLOs.

Most CD4$^+$ T cells in the paracortex are central memory or naive cells and are susceptible to HIV/SIV infection only upon activation. For example, these T cells may be activated by macrophages in the subcapsular sinus and medulla, which sense invading microbes transported via lymphatic networks by pattern recognition receptors that recognize pathogen-associated molecular patterns (PAMPs). Since PAMPs are present in glycans and/or glycolipids of microbes (23, 55), macrophages might sense differently SIVmac239 from Δ5G due to differences in the glycosylation, eliciting a robust inflammatory response against the former but not the latter. Alternatively, DCs/macrophages may capture and transfer HIV-1 to CD4$^+$ T cells via synaptic cell-to-cell interaction (transinfection) through C-type lectin receptors (DC-SIGN) and siglec-1 (CD169) (56, 57).

A recent study of SIV-infected rhesus macaques demonstrated the formation of reservoirs (latently infected cells) as early as 3 days p.i., even before the detection of plasma viral loads (58). In contrast, we have failed to detect any viral reservoirs in Δ5G-infected animals in late stages. Instead, the infected cells gradually disappeared following primary infection and became undetectable over time (unpublished results). Thus, levels of the reservoirs appear to inversely correlate with set point viral loads or with containment of the infection following primary infection. Recent studies demonstrated that Tfh cells are reservoirs in elite controllers of SIV infection and in HIV-infected patients with undetectable viral loads by combination antiretroviral therapy (cART) (59). Similarly, the live-attenuated ΔNef virus was found to target Tfh cells in B cell follicles in SLOs (10), suggesting that Tfh-specific infections are generally well contained. However, the viral load in Δ5G-infected animals was markedly lower than that in ΔNef-infected animals (11, 13), implying that Δ5G targets a different subset of CD4$^+$ T cells. Indeed, SIVmac239 and Δ5G are already known to preferentially infect different T cell subsets, as noted previously (1). Taken together, the data indicate that SIVmac239, ΔNef, and Δ5G elicit distinct host immune responses that depend on specific CD4$^+$ T cell subsets, which are then exclusively activated and become susceptible to infection (Fig. 9B).

Thus, future studies are needed to identify which CD4$^+$ T cell subsets are susceptible to Δ5G and to elucidate the mechanism by which glycosylation drives the specificity of SIVmac239 and Δ5G for distinct CD4$^+$ T cell subsets. Such studies may provide further insights into the pathogenesis and containment of early-stage HIV infections, as well as new opportunities to develop better vaccines and therapeutics.

MATERIALS AND METHODS

Viruses. Δ5G was derived by site-directed mutagenesis of an SIVmac239 infectious DNA clone in which the asparagine residues in the N-glycosylation sites at amino acids (aa) 79, 146, 171, 460, and 479 in gp120 were replaced with glutamine residues (12). Stocks of SIVmac239 and Δ5G were then prepared by transfection of proviral DNAs into 293T cells and propagated in phytohemagglutinin-stimulated PBMCs from rhesus macaques, as previously described (1, 11, 13).

Animals and ethics statement. Juvenile male rhesus macaques 2 to 7 years old and of Burmese origin were screened and found negative for SIV, simian T cell lymphotropic virus, herpes B virus, and type D retrovirus. The animals were housed individually and cared for according to the rules and guidelines for experimental animal welfare by the National Institute of Infectious Diseases and National Institute of Biomedical Innovation, Japan. The study was reviewed and approved by the Institutional Animal Care and Use Committees at the National Institute of Infectious Diseases and National Institute of Biomedical Innovation (protocol 606009), in accordance with the recommendations of the Weatherall report.

The animals were fed monkey diet supplemented with fresh fruit and water, and animal health was monitored daily and documented by animal care and veterinary staff. All efforts were expended to minimize suffering. These efforts included improvement of housing conditions, where possible, adopting of early endpoints, frequent monitoring of viral loads and immunological parameters, and humane euthanasia by barbiturate overdose once clinical AIDS or signs of fatal disease were noted.

Viral loads. The levels of SIV infection were monitored by measuring the plasma viral RNA loads using a highly sensitive quantitative real-time RT-PCR as described previously (1, 13). Briefly, viral RNA was isolated from plasma using a MagNA PureCompact Nucleic Acid Isolation kit (Roche Diagnostics). Real-time RT-PCR was performed using a QuantiTec Probe RT-PCR kit (Qiagen) and a Sequence Detection System (SDS) 7000 (Applied Biosystems). SIVmac239 *gag* was amplified with the probe 5′-FAM-TGTCC

ACCTGCCATTAAGTCCCGA-TAMRA-3′ (where FAM is 6-carboxyfluorescein and TAMRA is 6-carbo-xytetramethylrhodamine) and the primers 5′-GCAGAGGAGGAAATTACCCAGTAC-3′ and 5′-CAATTTTACC CAGGCATTTAATGTT-3′. The limit of detection was calculated to be 100 viral RNA copies per milliliter.

Immune cells. PBMCs and immune cells from spleens and mesenteric and inguinal LNs were collected from the following animals (all male) as previously reported (1, 13). The Δ5G group consisted of 15 animals (Mm0301, Mm0303, Mm0306, Mm0307, Mm0401, Mm0402, Mm0511, Mm0512, Mm0513, Mm0517, Mm0518, Mm0610, Mm0612, Mm0624, and Mm0625); the SIVmac239 group consisted of nine animals (Mm0403, Mm0405, Mm0406, Mm0519 [3 years], Mm0521, Mm0522, Mm0608, Mm0609, and Mm0611); the uninfected group consisted of three animals (Mm0127, Mm0308, and Mm0407).

Flow cytometry and cell sorting. Cryopreserved PBMCs and immune cells prepared from the spleen and the inguinal and mesenteric lymph nodes from the animals were analyzed and sorted by flow cytometry on a FACSAria (BD Biosciences) using fluorescein isothiocyanate (FITC)/Alexa Fluor 488, phycoerythrin (PE), energy-coupled dye (ECD), peridinin chlorophyll protein (PerCP)-Cy5.5, PE-Cy7, allophycocyanin (APC), Alexa Fluor 700, APC-Cy7, Pacific Blue, and BD Horizon V500 as fluorescent probes. Fluorochrome-conjugated MAb against CD4 (L200), CD3 (SP34-2), CD8 (SK1), CD95 (DX2), CD20 (L27), CCR5 (3A9), CXCR3 (1C6/CXCR3), CD16 (3G8), and major histocompatibility complex class II (MHC-II) DR (L243) were obtained from BD Biosciences. MAbs RMO52 (CD14), B9E9 (CD20), CD28.2 (CD28), and Z199 (NKG2A) were obtained from Beckmann Coulter, while MAbs M1/70 (CD11b) and J034D6 (CXCL10) were obtained from BioLegend. A MAb against MAC387 (MAC387) was purchased from Bio-Rad, while DAPI was obtained from Sigma-Aldrich. Data were analyzed in FlowJo, version 9.7.6 (Tree Star). Absolute counts of immune cells in blood were determined on an F820 automated hematology analyzer (Sysmex, Kobe, Japan).

ELISA for CXCL10. Plasma samples were collected from the animals reported previously, and plasma CXCL10 was measured with an enzyme-linked immunosorbent assay (ELISA) kit for human CXCL10 that cross-reacts with rhesus CXCL10 (BioLegend).

Microarray analyses. The PBMC samples utilized for the microarray analyses were derived from the animals that were described in previous studies (1, 13). Thus, six animals from the Δ5G group (all male; Mm0301 [5 years of age], Mm0303 [5 years], Mm0307 [5 years], Mm0512 [3 years], Mm0516 [3 years], and Mm0513 [3 years]) were intravenously inoculated with 100 50% tissue culture infective doses (TCID$_{50}$) of the deglycosylated mutant described previously (13). In the SIVmac239-infected group, three of the animals (all male; Mm9702 [3 years], Mm9715 [3 years], and Mm0914 [6 years]), were intravenously infected using 100 TCID$_{50}$, and the other three animals (all male; Mm0403 [4 years], Mm0609 [2 years], and Mm0611 [2 years]) were infected using 300 TCID$_{50}$ of SIVmac239 as described previously (1). The PBMCs from six normal healthy monkeys (all male; Mm9702 [3 years], Mm9715 [3 years], Mm0307 [5 years], Mm0516 [3 years], Mm0518 [3 years], and Mm0402 [4 years]) were used as the uninfected group.

RNA was prepared from cryopreserved PBMCs using a commercial total RNA isolation kit (RNeasy minikit; Qiagen), and the quality and concentration were assessed using a Bioanalyzer 2100 (Agilent Technologies) using an RNA 6000 Nano kit (Agilent) and an ND-1000 spectrophotometer (NanoDrop Technology), respectively. Next, 100 ng of RNA was amplified and labeled using a low-RNA-input linear amplification kit (Agilent) and then hybridized to a rhesus monkey microarray (version 2; Agilent Technologies) as previously described (60). The slides were scanned with a DNA microarray scanner (Agilent Technologies). Images were analyzed using Feature extraction software (Agilent Technologies). The data were analyzed using the Subio platform (Subio, Kagoshima, Japan). Briefly, the text file exported by Future Extraction was imported into the Subio platform. The raw data were normalized per chip to the 75th percentile expression level. The sample data were subjected to normalization per gene to the median expression level of all samples. The samples were classified into three groups (SIVmac239-infected animals, Δ5G-infected animals, and uninfected animals). All data are presented as the mean per group. The genes that showed significant differences between the two of three groups (SIVmac239- and Δ5G-infected animals, SIVmac239-infected and uninfected animals, or Δ5G-infected and uninfected animals) were identified using the Subio platform. To examine gene expression signatures associated with SIVmac239 and Δ5G infection, we performed two hierarchical clustering analyses: (i) the genes were selected by the significant differences by the criteria of fold change of >2 or <0.5 and P value of <0.05 among three group described above; (ii) the selected genes were sorted by gene functions such as type I interferon-stimulated genes (ISGs), genes of antiretroviral host factors, pattern recognition receptors, and the related genes, genes of inflammatory responses, Th1 cell activation, and Th1 differentiation, and genes of chemokines and chemokine receptors, whereas some genes in the categories other than ISGs have Gene Ontology (GO) terms associated with the interferon response.

qRT-PCR. RNA was prepared, using an RNeasy minikit (Qiagen), from PBMCs and from the cells sorted by flow cytometry. Gene expression was quantified by qRT-PCR on a LightCycler 480 (Roche Applied Science) using a One-Step PrimeScript RT-PCR kit (TaKaRa Bio, Shiga, Japan) and primers from Integrated DNA Technologies. CXCL10 was amplified with the double-quenched probe 5′-GAGGTGTCTGAATCCAG AATCTAAGGCC-3′, sense primer 5′-CCACATGTTGAGATCATTGC-3′, and antisense primer 5′-TAGACCTTT CCTTGCTAACTGC-3′. CXCL11 was amplified with 5′-TAGGCCCTGGAGTAAAAGCAGTGAAAGT-3′, 5′-TGTG TACTACGGTTGTTCAAGG-3′, and 5′-GGAGGCTTTCTCAATATCTGC-3′ as probe, sense primer, and antisense primer, respectively. CXCL9 was amplified with 5′-TCAACACCAACCAAGGGACTATCCACCT AC-3′, 5′-AATGAGGAAGGGTCGCTGTTC-3′, and 5′-TTTGGAGCAAATTGTTTAAGGTCTT-3′ as probe, sense primer, and antisense primer, respectively. CCL8 was amplified with 5′-CCACAGGGACTTGCT CAGCCAGATTC-3′, 5′-CTCATGGCAGCCACTTTCAG-3′, and 5′-AGCAGGTGATTGGAATGGAAAC-3′ as probe, sense primer, and antisense primer, respectively. Finally, glyceraldehyde-3-phosphate dehydrogenase (GAPDH) was amplified with 5′-AGCGACACCCACTCTTCCACCTTCG-3′, 5′-GGTGGTCTCCT

CCGACTTCA-3′, and 5′-GTGGTCGTTGAGGGCAATG-3′ as probe, sense primer, and antisense primer, respectively. Expression of target genes was calculated from quantification cycle (C_q) values and is reported as relative expression units normalized to the level of GAPDH.

Statistical analysis. Data were analyzed by a Mann-Whiney test and Spearman correlation test in GraphPad Prism, version 4.0, and significant differences among groups are indicated on the figures.

ACKNOWLEDGMENTS

REFERENCES

1. Sugimoto C, Nakamura S, Hagen SI, Tsunetsugu-Yokota Y, Villinger F, Ansari AA, Suzuki Y, Yamamoto N, Nagai Y, Picker LJ, Mori K. 2012. Glycosylation of simian immunodeficiency virus influences immune-tissue targeting during primary infection, leading to immunodeficiency or viral control. J Virol 86:9323–9336. https://doi.org/10.1128/JVI.00948-12.

2. Mattapallil JJ, Douek DC, Hill B, Nishimura Y, Martin M, Roederer M. 2005. Massive infection and loss of memory CD4+ T cells in multiple tissues during acute SIV infection. Nature 434:1093–1097. https://doi.org/10.1038/nature03501.

3. O'Shea JJ, Paul WE. 2010. Mechanisms underlying lineage commitment and plasticity of helper CD4+ T cells. Science 327:1098–1102. https://doi.org/10.1126/science.1178334.

4. Brenchley JM, Paiardini M, Knox KS, Asher AI, Cervasi B, Asher TE, Scheinberg P, Price DA, Hage CA, Kholi LM, Khoruts A, Frank I, Else J, Schacker T, Silvestri G, Douek DC. 2008. Differential Th17 CD4 T-cell depletion in pathogenic and nonpathogenic lentiviral infections. Blood 112:2826–2835. https://doi.org/10.1182/blood-2008-05-159301.

5. El Hed A, Khaitan A, Kozhaya L, Manel N, Daskalakis D, Borkowsky W, Valentine F, Littman DR, Unutmaz D. 2010. Susceptibility of human Th17 cells to human immunodeficiency virus and their perturbation during infection. J Infect Dis 201:843–854. https://doi.org/10.1086/651021.

6. Moreno-Fernandez ME, Zapata W, Blackard JT, Franchini G, Chougnet CA. 2009. Human regulatory T cells are targets for human immunodeficiency virus (HIV) infection, and their susceptibility differs depending on the HIV type 1 strain. J Virol 83:12925–12933. https://doi.org/10.1128/JVI.01352-09.

7. Brenchley JM, Vinton C, Tabb B, Hao XP, Connick E, Paiardini M, Lifson JD, Silvestri G, Estes JD. 2012. Differential infection patterns of CD4+ T cells and lymphoid tissue viral burden distinguish progressive and nonprogressive lentiviral infections. Blood 120:4172–4181. https://doi.org/10.1182/blood-2012-06-437608.

8. Connick E, Folkvord JM, Lind KT, Rakasz EG, Miles B, Wilson NA, Santiago ML, Schmitt K, Stephens EB, Kim HO, Wagstaff R, Li S, Abdelaal HM, Kemp N, Watkins DI, MaWhinney S, Skinner PJ. 2014. Compartmentalization of simian immunodeficiency virus replication within secondary lymphoid tissues of rhesus macaques is linked to disease stage and inversely related to localization of virus-specific CTL. J Immunol 193:5613–5625. https://doi.org/10.4049/jimmunol.1401161.

9. Fukazawa Y, Lum R, Okoye AA, Park H, Matsuda K, Bae JY, Hagen SI, Shoemaker R, Deleage C, Lucero C, Morcock D, Swanson T, Legasse AW, Axthelm MK, Hesselgesser J, Geleziunas R, Hirsch VM, Edlefsen PT, Piatak M, Jr, Estes JD, Lifson JD, Picker LJ. 2015. B cell follicle sanctuary permits persistent productive simian immunodeficiency virus infection in elite controllers. Nat Med 21:132–139. https://doi.org/10.1038/nm.3781.

10. Sugimoto C, Tadakuma K, Otani I, Moritoyo T, Akari H, Ono F, Yoshikawa Y, Sata T, Izumo S, Mori K. 2003. *nef* gene is required for robust productive infection by simian immunodeficiency virus of T-cell-rich

paracortex in lymph nodes. J Virol 77:4169–4180. https://doi.org/10.1128/JVI.77.7.4169-4180.2003.

11. Mori K, Yasutomi Y, Ohgimoto S, Nakasone T, Takamura S, Shioda T, Nagai Y. 2001. Quintuple deglycosylation mutant of simian immunodeficiency virus SIVmac239 in rhesus macaques: robust primary replication, tightly contained chronic infection, and elicitation of potent immunity against the parental wild-type strain. J Virol 75:4023–4028. https://doi.org/10.1128/JVI.75.9.4023-4028.2001.

12. Ohgimoto S, Shioda T, Mori K, Nakayama EE, Hu H, Nagai Y. 1998. Location-specific, unequal contribution of the N glycans in simian immunodeficiency virus gp120 to viral infectivity and removal of multiple glycans without disturbing infectivity. J Virol 72:8365–8370.

13. Sugimoto C, Watanabe S, Naruse T, Kajiwara E, Shiino T, Umano N, Ueda K, Sato H, Ohgimoto S, Hirsch V, Villinger F, Ansari AA, Kimura A, Miyazawa M, Suzuki Y, Yamamoto N, Nagai Y, Mori K. 2010. Protection of macaques with diverse MHC genotypes against a heterologous SIV by vaccination with a deglycosylated live-attenuated SIV. PLoS One 5:e11678. https://doi.org/10.1371/journal.pone.0011678.

14. Sugimoto C, Nakayama EE, Shioda T, Villinger F, Ansari AA, Yamamoto N, Suzuki Y, Nagai Y, Mori K. 2008. Impact of glycosylation on antigenicity of simian immunodeficiency virus SIV239: induction of rapid V1/V2-specific non-neutralizing antibody and delayed neutralizing antibody following infection with an attenuated deglycosylated mutant. J Gen Virol 89:554–566. https://doi.org/10.1099/vir.0.83186-0.

15. Stacey AR, Norris PJ, Qin L, Haygreen EA, Taylor E, Heitman J, Lebedeva M, DeCamp A, Li D, Grove D, Self SG, Borrow P. 2009. Induction of a striking systemic cytokine cascade prior to peak viremia in acute human immunodeficiency virus type 1 infection, in contrast to more modest and delayed responses in acute hepatitis B and C virus infections. J Virol 83:3719–3733. https://doi.org/10.1128/JVI.01844-08.

16. Lederer S, Favre D, Walters KA, Proll S, Kanwar B, Kasakow Z, Baskin CR, Palermo R, McCune JM, Katze MG. 2009. Transcriptional profiling in pathogenic and non-pathogenic SIV infections reveals significant distinctions in kinetics and tissue compartmentalization. PLoS Pathog 5:e1000296. https://doi.org/10.1371/journal.ppat.1000296.

17. Jacquelin B, Mayau V, Targat B, Liovat AS, Kunkel D, Petitjean G, Dillies MA, Roques P, Butor C, Silvestri G, Giavedoni LD, Lebon P, Barre-Sinoussi F, Benecke A, Muller-Trutwin MC. 2009. Nonpathogenic SIV infection of African green monkeys induces a strong but rapidly controlled type I IFN response. J Clin Invest 119:3544–3555. https://doi.org/10.1172/JCI40093.

18. Bosinger SE, Li Q, Gordon SN, Klatt NR, Duan L, Xu L, Francella N, Sidahmed A, Smith AJ, Cramer EM, Zeng M, Masopust D, Carlis JV, Ran L, Vanderford TH, Paiardini M, Isett RB, Baldwin DA, Else JG, Staprans SI, Silvestri G, Haase AT, Kelvin DJ. 2009. Global genomic analysis reveals rapid control of a robust innate response in SIV-infected sooty mangabeys. J Clin Invest 119:3556–3572. https://doi.org/10.1172/JCI40115.

19. Schoggins JW, Wilson SJ, Panis M, Murphy MY, Jones CT, Bieniasz P, Rice CM. 2011. A diverse range of gene products are effectors of the type I

interferon antiviral response. Nature 472:481–485. https://doi.org/10.1038/nature09907.

20. Goubau D, Deddouche S, Reis e Sousa C. 2013. Cytosolic sensing of viruses. Immunity 38:855–869. https://doi.org/10.1016/j.immuni.2013.05.007.

21. Lepelley A, Louis S, Sourisseau M, Law HK, Pothlichet J, Schilte C, Chaperot L, Plumas J, Randall RE, Si-Tahar M, Mammano F, Albert ML, Schwartz O. 2011. Innate sensing of HIV-infected cells. PLoS Pathog 7:e1001284. https://doi.org/10.1371/journal.ppat.1001284.

22. Han X, Li X, Yue SC, Anandaiah A, Hashem F, Reinach PS, Koziel H, Tachado SD. 2012. Epigenetic regulation of tumor necrosis factor alpha (TNFα) release in human macrophages by HIV-1 single-stranded RNA (ssRNA) is dependent on TLR8 signaling. J Biol Chem 287:13778–13786. https://doi.org/10.1074/jbc.M112.342683.

23. Takeuchi O, Akira S. 2010. Pattern recognition receptors and inflammation. Cell 140:805–820. https://doi.org/10.1016/j.cell.2010.01.022.

24. Iwasaki A, Medzhitov R. 2010. Regulation of adaptive immunity by the innate immune system. Science 327:291–295. https://doi.org/10.1126/science.1183021.

25. Monroe KM, Yang Z, Johnson JR, Geng X, Doitsh G, Krogan NJ, Greene WC. 2014. IFI16 DNA sensor is required for death of lymphoid CD4 T cells abortively infected with HIV. Science 343:428–432. https://doi.org/10.1126/science.1243640.

26. Sung JH, Zhang H, Moseman EA, Alvarez D, Iannacone M, Henrickson SE, de la Torre JC, Groom JR, Luster AD, von Andrian UH. 2012. Chemokine guidance of central memory T cells is critical for antiviral recall responses in lymph nodes. Cell 150:1249–1263. https://doi.org/10.1016/j.cell.2012.08.015.

27. Groom JR, Richmond J, Murooka TT, Sorensen EW, Sung JH, Bankert K, von Andrian UH, Moon JJ, Mempel TR, Luster AD. 2012. CXCR3 chemokine receptor-ligand interactions in the lymph node optimize CD4$^+$ T helper 1 cell differentiation. Immunity 37:1091–1103. https://doi.org/10.1016/j.immuni.2012.08.016.

28. Kurachi M, Kurachi J, Suenaga F, Tsukui T, Abe J, Ueha S, Tomura M, Sugihara K, Takamura S, Kakimi K, Matsushima K. 2011. Chemokine receptor CXCR3 facilitates CD8$^+$ T cell differentiation into short-lived effector cells leading to memory degeneration. J Exp Med 208:1605–1620. https://doi.org/10.1084/jem.20102101.

29. de la Fuente H, Cibrian D, Sanchez-Madrid F. 2012. Immunoregulatory molecules are master regulators of inflammation during the immune response. FEBS Lett 586:2897–2905. https://doi.org/10.1016/j.febslet.2012.07.032.

30. Salvador JM, Mittelstadt PR, Belova GI, Fornace AJ, Jr, Ashwell JD. 2005. The autoimmune suppressor Gadd45α inhibits the T cell alternative p38 activation pathway. Nat Immunol 6:396–402. https://doi.org/10.1038/ni1176.

31. Yang J, Zhu H, Murphy TL, Ouyang W, Murphy KM. 2001. IL-18-stimulated GADD45β required in cytokine-induced, but not TCR-induced, IFN-γ production. Nat Immunol 2:157–164. https://doi.org/10.1038/84264.

32. Lu B, Yu H, Chow C, Li B, Zheng W, Davis RJ, Flavell RA. 2001. GADD45γ mediates the activation of the p38 and JNK MAP kinase pathways and cytokine production in effector TH1 cells. Immunity 14:583–590. https://doi.org/10.1016/S1074-7613(01)00141-8.

33. Yan N, Chen ZJ. 2012. Intrinsic antiviral immunity. Nat Immunol 13:214–222. https://doi.org/10.1038/ni.2229.

34. Chang HC, Han L, Goswami R, Nguyen ET, Pelloso D, Robertson MJ, Kaplan MH. 2009. Impaired development of human Th1 cells in patients with deficient expression of STAT4. Blood 113:5887–5890. https://doi.org/10.1182/blood-2008-09-179820.

35. Zlotnik A, Yoshie O. 2012. The chemokine superfamily revisited. Immunity 36:705–716. https://doi.org/10.1016/j.immuni.2012.05.008.

36. Shi C, Pamer EG. 2011. Monocyte recruitment during infection and inflammation. Nat Rev Immunol 11:762–774. https://doi.org/10.1038/nri3070.

37. Ziegler-Heitbrock L. 2007. The CD14$^+$ CD16$^+$ blood monocytes: their role in infection and inflammation. J Leukoc Biol 81:584–592.

38. Ginhoux F, Jung S. 2014. Monocytes and macrophages: developmental pathways and tissue homeostasis. Nat Rev Immunol 14:392–404. https://doi.org/10.1038/nri3671.

39. Zawada AM, Rogacev KS, Rotter B, Winter P, Marell RR, Fliser D, Heine GH. 2011. SuperSAGE evidence for CD14$^+$ CD16$^+$ monocytes as a third monocyte subset. Blood 118:e50–e61. https://doi.org/10.1182/blood-2011-01-326827.

40. Hyrcza MD, Kovacs C, Loutfy M, Halpenny R, Heisler L, Yang S, Wilkins O,

Ostrowski M, Der SD. 2007. Distinct transcriptional profiles in ex vivo CD4$^+$ and CD8$^+$ T cells are established early in human immunodeficiency virus type 1 infection and are characterized by a chronic interferon response as well as extensive transcriptional changes in CD8$^+$ T cells. J Virol 81:3477–3486. https://doi.org/10.1128/JVI.01552-06.

41. Soulas C, Conerly C, Kim WK, Burdo TH, Alvarez X, Lackner AA, Williams KC. 2011. Recently infiltrating MAC387$^+$ monocytes/macrophages a third macrophage population involved in SIV and HIV encephalitic lesion formation. Am J Pathol 178:2121–2135. https://doi.org/10.1016/j.ajpath.2011.01.023.

42. Otani I, Mori K, Sata T, Terao K, Doi K, Akari H, Yoshikawa Y. 1999. Accumulation of MAC387$^+$ macrophages in paracortical areas of lymph nodes in rhesus monkeys acutely infected with simian immunodeficiency virus. Microbes Infect 1:977–985. https://doi.org/10.1016/S1286-4579(99)80515-2.

43. Kawai T, Akira S. 2011. Toll-like receptors and their crosstalk with other innate receptors in infection and immunity. Immunity 34:637–650. https://doi.org/10.1016/j.immuni.2011.05.006.

44. Deeks SG, Tracy R, Douek DC. 2013. Systemic effects of inflammation on health during chronic HIV infection. Immunity 39:633–645. https://doi.org/10.1016/j.immuni.2013.10.001.

45. Genesca M, Ma ZM, Wang Y, Assaf B, Qureshi H, Fritts L, Huang Y, McChesney MB, Miller CJ. 2012. Live-attenuated lentivirus immunization modulates innate immunity and inflammation while protecting rhesus macaques from vaginal simian immunodeficiency virus challenge. J Virol 86:9188–9200. https://doi.org/10.1128/JVI.00532-12.

46. Paiardini M, Cervasi B, Reyes-Aviles E, Micci L, Ortiz AM, Chahroudi A, Vinton C, Gordon SN, Bosinger SE, Francella N, Hallberg PL, Cramer E, Schlub T, Chan ML, Riddick NE, Collman RG, Apetrei C, Pandrea I, Else J, Munch J, Kirchhoff F, Davenport MP, Brenchley JM, Silvestri G. 2011. Low levels of SIV infection in sooty mangabey central memory CD4$^+$ T cells are associated with limited CCR5 expression. Nat Med 17:830–836. https://doi.org/10.1038/nm.2395.

47. Chahroudi A, Bosinger SE, Vanderford TH, Paiardini M, Silvestri G. 2012. Natural SIV hosts: showing AIDS the door. Science 335:1188–1193. https://doi.org/10.1126/science.1217550.

48. Hasegawa A, Liu H, Ling B, Borda JT, Alvarez X, Sugimoto C, Vinet-Oliphant H, Kim WK, Williams KC, Ribeiro RM, Lackner AA, Veazey RS, Kuroda MJ. 2009. The level of monocyte turnover predicts disease progression in the macaque model of AIDS. Blood 114:2917–2925. https://doi.org/10.1182/blood-2009-02-204263.

49. Klatt NR, Funderburg NT, Brenchley JM. 2013. Microbial translocation, immune activation, and HIV disease. Trends Microbiol 21:6–13. https://doi.org/10.1016/j.tim.2012.09.001.

50. Khan IA, MacLean JA, Lee FS, Casciotti L, DeHaan E, Schwartzman JD, Luster AD. 2000. IP-10 is critical for effector T cell trafficking and host survival in *Toxoplasma gondii* infection. Immunity 12:483–494. https://doi.org/10.1016/S1074-7613(00)80200-9.

51. Liu MT, Chen BP, Oertel P, Buchmeier MJ, Armstrong D, Hamilton TA, Lane TE. 2000. The T cell chemoattractant IFN-inducible protein 10 is essential in host defense against viral-induced neurologic disease. J Immunol 165:2327–2330. https://doi.org/10.4049/jimmunol.165.5.2327.

52. Yoneyama H, Narumi S, Zhang Y, Murai M, Baggiolini M, Lanzavecchia A, Ichida T, Asakura H, Matsushima K. 2002. Pivotal role of dendritic cell-derived CXCL10 in the retention of T helper cell 1 lymphocytes in secondary lymph nodes. J Exp Med 195:1257–1266. https://doi.org/10.1084/jem.20011983.

53. Ancuta P, Wang J, Gabuzda D. 2006. CD16$^+$ monocytes produce IL-6, CCL2, and matrix metalloproteinase-9 upon interaction with CX3CL1-expressing endothelial cells. J Leukoc Biol 80:1156–1164. https://doi.org/10.1189/jlb.0206125.

54. Antonelli LR, Leoratti FM, Costa PA, Rocha BC, Diniz SQ, Tada MS, Pereira DB, Teixeira-Carvalho A, Golenbock DT, Goncalves R, Gazzinelli RT. 2014. The CD14$^+$ CD16$^+$ inflammatory monocyte subset displays increased mitochondrial activity and effector function during acute *Plasmodium vivax* malaria. PLoS Pathog 10:e1004393. https://doi.org/10.1371/journal.ppat.1004393.

55. Sewald X, Ladinsky MS, Uchil PD, Beloor J, Pi R, Herrmann C, Motamedi N, Murooka TT, Brehm MA, Greiner DL, Shultz LD, Mempel TR, Bjorkman PJ, Kumar P, Mothes W. 2015. Retroviruses use CD169-mediated trans-infection of permissive lymphocytes to establish infection. Science 350:563–567. https://doi.org/10.1126/science.aab2749.

56. Geijtenbeek TB, Kwon DS, Torensma R, van Vliet SJ, van Duijnhoven GC,

Middel J, Cornelissen IL, Nottet HS, KewalRamani VN, Littman DR, Figdor CG, van Kooyk Y. 2000. DC-SIGN, a dendritic cell-specific HIV-1-binding protein that enhances trans-infection of T cells. Cell 100:587–597. https://doi.org/10.1016/S0092-8674(00)80694-7.

57. Izquierdo-Useros N, Lorizate M, McLaren PJ, Telenti A, Krausslich HG, Martinez-Picado J. 2014. HIV-1 capture and transmission by dendritic cells: the role of viral glycolipids and the cellular receptor Siglec-1. PLoS Pathog 10:e1004146. https://doi.org/10.1371/journal.ppat.1004146.

58. Whitney JB, Hill AL, Sanisetty S, Penaloza-MacMaster P, Liu J, Shetty M, Parenteau L, Cabral C, Shields J, Blackmore S, Smith JY, Brinkman AL, Peter LE, Mathew SI, Smith KM, Borducchi EN, Rosenbloom DI, Lewis MG, Hattersley J, Li B, Hesselgesser J, Geleziunas R, Robb ML, Kim JH, Michael NL, Barouch DH. 2014. Rapid seeding of the viral reservoir prior to SIV

viraemia in rhesus monkeys. Nature 512:74–77. https://doi.org/10.1038/nature13594.

59. Banga R, Procopio FA, Noto A, Pollakis G, Cavassini M, Ohmiti K, Corpataux JM, de Leval L, Pantaleo G, Perreau M. 2016. PD-1+ and follicular helper T cells are responsible for persistent HIV-1 transcription in treated aviremic individuals. Nat Med 22:754–761. https://doi.org/10.1038/nm.4113.

60. Iwata-Yoshikawa N, Uda A, Suzuki T, Tsunetsugu-Yokota Y, Sato Y, Morikawa S, Tashiro M, Sata T, Hasegawa H, Nagata N. 2014. Effects of Toll-like receptor stimulation on eosinophilic infiltration in lungs of BALB/c mice immunized with UV-inactivated severe acute respiratory syndrome-related coronavirus vaccine. J Virol 88:8597–85614. https://doi.org/10.1128/JVI.00983-14.